Nucleation in the Theophylline:Glutaric acid cocrystal system

Hannah McTague[1] and Åke C. Rasmuson*[1,2]

[1]*Synthesis and Solid State Pharmaceutical Centre (SSPC), Bernal Institute, Department of Chemical and Environmental Science, University of Limerick. Limerick V94 T9PX, Ireland.*

[2]*Department of Chemical Engineering and Technology, KTH Royal Institute of Technology, SE-100 44 Stockholm, Sweden.*

Characterisation

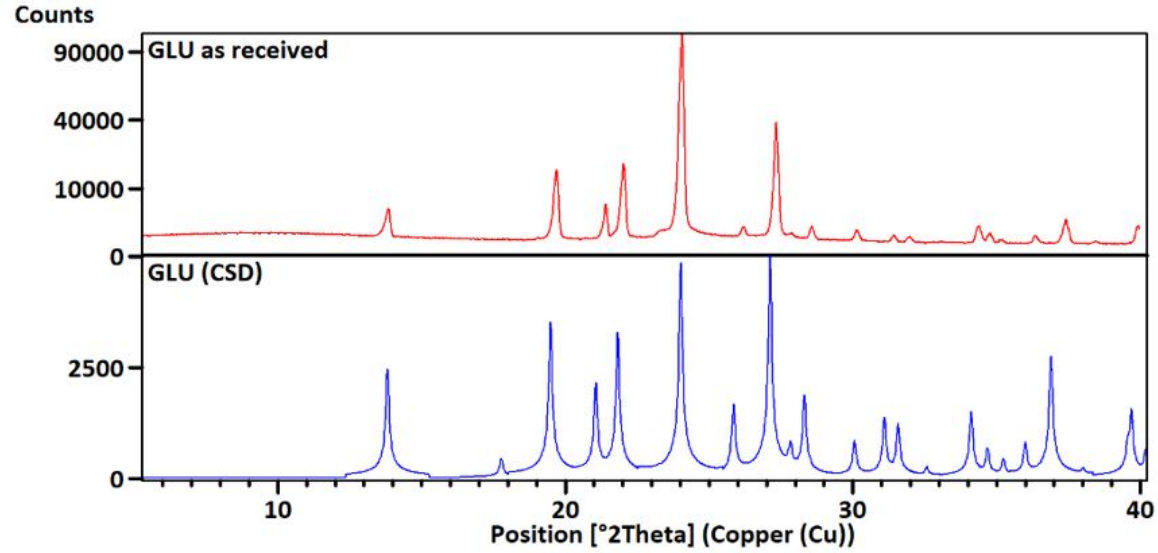

Figure 1 PXRD of glutaric acid as received versus β-glutaric acid structure from the CSD.

As seen in the diffractogram in **Figure 1** GLU as received matches the pattern of GLU entered previously in the CSD for the β-polymorph form with ref. code GLURAC.

The DSC graph in **Figure 2** shows the endotherm peak of THP II at 275 °C and β-GLU at 97 °C for the α-polymorph with a transition from β to α at 74 °C. In the present work the β-glutaric acid form is used. In the DSC graph for the THP:GLU cocrystal, decomposition of the cocrystal is observed at 120 °C which is between the melting point of both components.

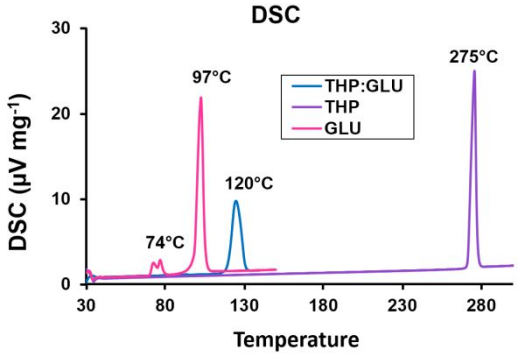

Figure 2 Heat flow data from DSC performed on THP:GLU 1:1 cocrystal, THP II and β-GLU.

Solid samples of pure THP:GLU cocrystal and pure THP II and β-GLU crystallised from chloroform were analysed by solid state Perkin Elmer ATR-IR.

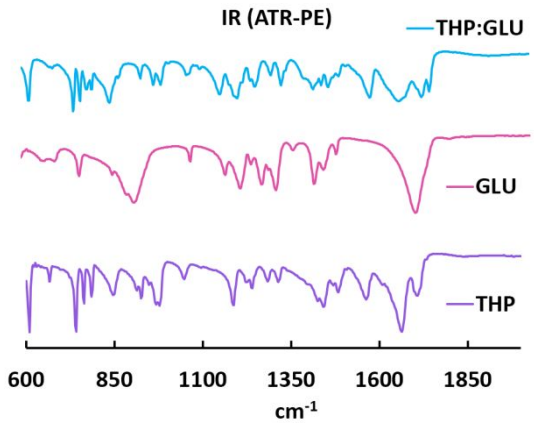

Figure 3 IR (ATR-PE) ν_{max}/cm^{-1}: 1673 (C=O).

The IR spectra obtained revealed a shift in the C=O peak outlined in **Table 1**. Raman spectra reveal a similar shift in the C=O group as seen in **Figure 4** and detailed in **Table 1**.

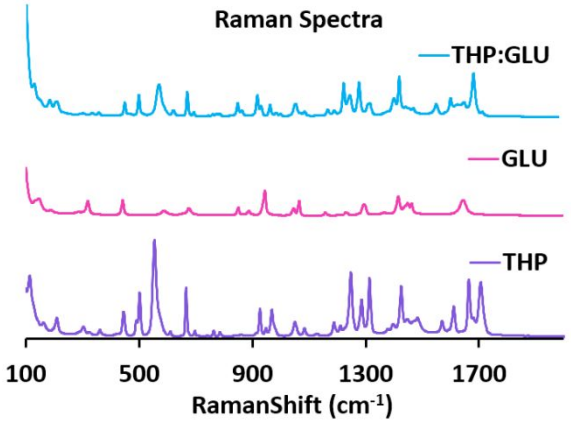

Figure 4 Raman Spectra obtained from solid samples of cocrystal and pure components using a Kaiser Raman probe.

Table 1 C=O peak shift for THP:GLU cocrystal observed by ATR-IR and solid-state Raman spectroscopy.

	IR	**Raman**
	ν_{CO}/cm^{-1}	cm^{-1}
THP:GLU	1644	1697
GLU	1688	1652
THP	1664	1708

Eutectic Point Determination

Two systems were created where the solid phase at equilibrium was a mixture of THP:GLU cocrystal and THP II for point E1 determination and a mixture of THP:GLU cocrystal with β-

GLU for point E2 determination. These were created at the 100 mL scale with starting compositions detailed in **Table 2**.

Table 2 Starting compositions for eutectic point determination. The composition in mole fraction (MF) of the starting systems have been plotted on the ternary phase diagram in **Figure 5.**

E1						
	THP:GLU	**THP**	**CLO**		**THPGLU**	
g	**1.2**	**1**	**148.9**		0.003843	**mol GLU**
mw	312.29	170.18	119.37		0.003843	**mol THP**
moles	0.003843	0.005876	1.247382			
MF	0.003057	0.004674	0.992269			
	THP	**GLU**	**CLO**			
mol	0.009719	0.003843	1.247382			
mr	180.17	132.12	119.37			
MF	0.007707	0.003047	0.989245			
E2						
	THPGLU	**GLU**	**CLO**		**THPGLU**	
g	**1**	**0.9**	**148.9**		0.003202	**mol THP**
mr	312.29	132.12	119.37		0.003202	**mol GLU**
mol	0.003202	0.006812	1.247382			
MF	0.002547	0.005418	0.992036			
	THP	GLU	CLO			
mol	0.003202	0.010014	1.247382			
mr	180.17	132.12	119.37			
MF	0.002540	0.007944	0.989516			

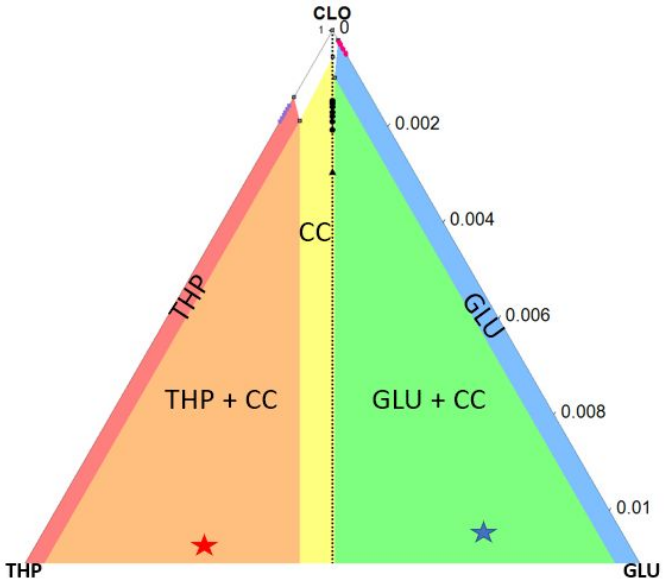

Figure 5 Schematic TPD of THP:GLU 1:1 cocrystal in chloroform at 10 °C. The mole fraction compositions of the starting systems for E1 and E2 eutectic point determination are marked with a red and blue star respectively.

E1 and E2 starting compositions were made in duplicate. These systems were labelled as E1 A, E1 B and E2 A, E2 B. A PTFE magnetic stir bar was added to each flask and the flasks were tightly sealed. The systems were placed in a 10 °C water bath and stirred at 400 rpm. E1 A and E2 A were sampled after 24 hours under these conditions and E1 B and E2 B were sampled after 48 hours. The samples were dried and re-constituted in acetonitrile. The liquid phase composition was then obtained utilising UV-vis analysis in combination with the gravimetric data from evaporation to dryness. Agitation was ceased and the phases were left to separate for 1 hour prior to sampling the liquid phase. Due to the high density of chloroform most of the solid phase accumulated at the top of the liquid phase. Some solid particles remained suspended throughout the bulk of the solution. The flask was then opened gently and replaced with a lid fitted with a rubber septum. A syringe with needle was used to penetrate the floating solid phase and sample the almost totally clear liquid phase below. The disturbance of the top layer by the needle caused some more solid to become dispersed in the solution but the best effort was made to isolate only clear liquid. The liquid was sampled through the needle using 20 mL syringes and filtered through 2 µm PTFE filters into pre-weighed 30 mL capacity vials. All apparatus used was at room temperature.

Three 20 mL samples of the liquid were taken from E1 A and E2 A (labelled as E1 A1, E1 A2 etc.) after 24 hours and the same was performed on E1 B and E2 B after 48 hours. The samples were weighed and then evaporated to dryness. Samples were determined to be dry after 7 days confirmed by weight consistency checks 24 hours apart and loss on drying experiments in an oven at 50 °C for 2 hours.

The concentration of solid to chloroform is calculated gravimetrically in g/g for all samples. Agreement between the g/g values for the samples taken from the 24 hour mixtures and the 48 hour mixtures means that equilibrium had been reached after 24 hours.

Table 3 Gravimetric analysis of samples taken from the liquid phase in eutectic point determination experiments. The solubility in g/g is g solute per g of chloroform solvent.

Sample	g/g	Avg g/g	Std. Dev.
E1 A1	0.00263	0.00263	1.17E-05
E1 A2	0.00262		
E1 A3	0.00265		
E1 B1	0.00261	0.00265	4.38E-05
E1 B2	0.00263		
E1 B3	0.00271		
E2 A1	0.00121	0.00123	1.12E-05
E2 A2	0.00124		
E2 A3	0.00123		
E2 B1	0.00125	0.00125	5.45E-06
E2 B2	0.00125		
E2 B3	0.00126		

After the sampling of the liquid phase the mixtures were filtered and the solid phase in equilibrium was analysed by PXRD. The solid was identified as a mixture of cocrystal and THP II for the E1 experiments, **Figure 6,** and a mixture of cocrystal and β-GLU for the E2 experiments, **Figure 7.**

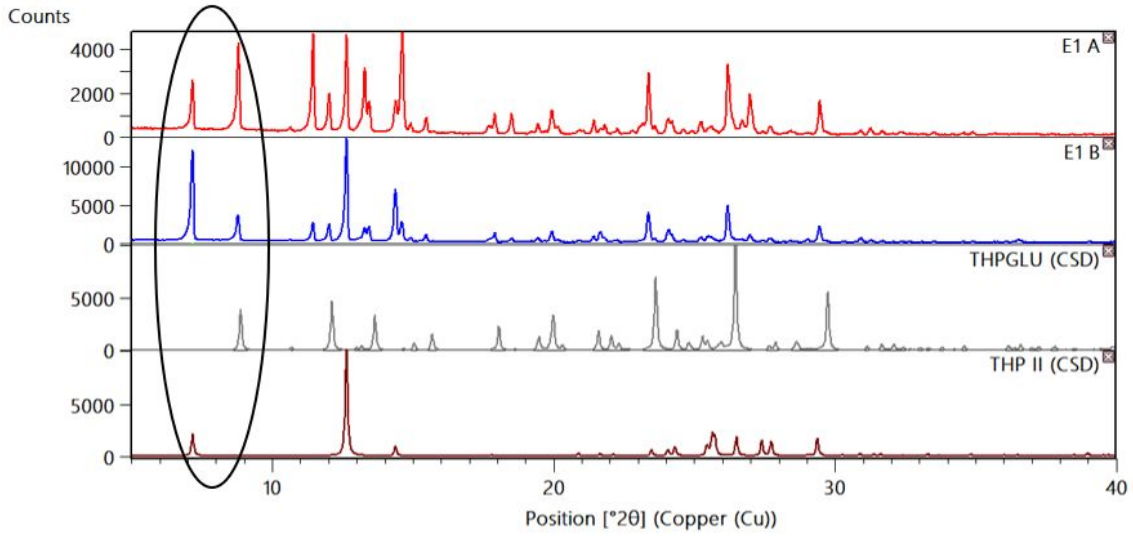

Figure 6 Diffractogram of solid phase in equilibrium with E1. Peaks of both THP:GLU 1:1 cocrystal and pure THP II are present.

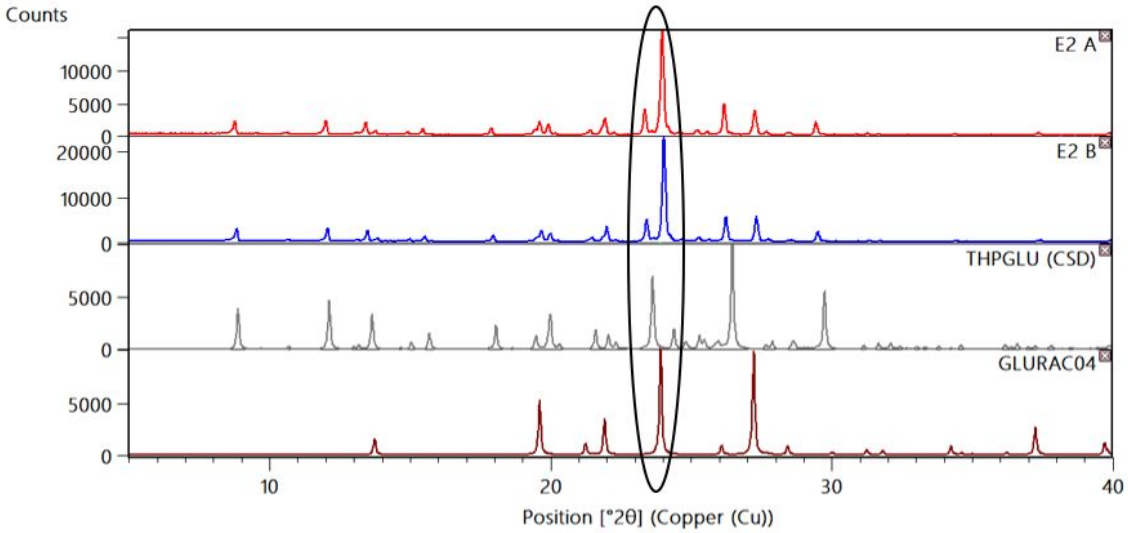

Figure 7 Diffractogram of solid phase in equilibrium with E2. Peaks of both THP:GLU 1:1 cocrystal and pure β- glutaric acid (GLURAC04) are present.

Samples E1 B3 and E2 B3 were filled with 35 mL MeCN and sonicated for 30 mins. The vials were placed in a water bath at 65 °C with stirring at 400 rpm using a PTFE stir bar for 24 hours. The solution was transferred to a 100 mL flask and a further 60 mL of MeCN was added. Upon reaching room temperature the appropriate dilutions were made and UV measurements at λ = 270 nm were taken.

The UV absorption of THP at 270 nm, is not completely independent of the concentration of GLU. Therefore, an iterative approach has been taken where the concentration of GLU in the calibration solutions is iteratively refined to eventually match the actual GLU concentration in the sample. Since there are different ratios of THP to GLU at the eutectic points E1 and E2, the calibration solutions are adjusted accordingly. Calibration curves were created using stock solutions of THP II (15 mg in 500 mL MeCN) and β-GLU (11 mg in 500 mL MeCN). The calibration curves of pure THP II and pure β-GLU in MeCN have been plotted in **Figure 8** and **Figure 9** respectively.

Table 4 Concentrations (mg/g) and absorbance for the calibration curve of pure THP II in MeCN.

Conc. mg/g	Abs.
0.015	0.599
0.013	0.533
0.012	0.456
0.010	0.377
0.008	0.300

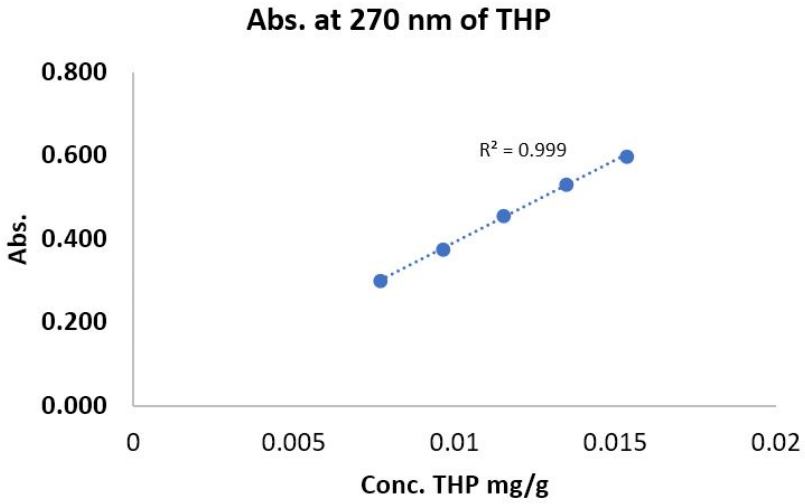

Figure 8 Calibration curve for pure THP in MeCN at λ= 270 nm.

The pure GLU solutions absorb minimally at the concentrations used in this work and the UV reading was well below the accurate range of the instrument even for the undiluted stock solution conc. = 0.03438 mg/g, **Table 5**.

Table 5 Concentrations and absorbance for calibration curve of pure GLU in MeCN.

Conc. mg/g	Abs.
0.010	0.011
0.017	0.019
0.024	0.026
0.034	0.034

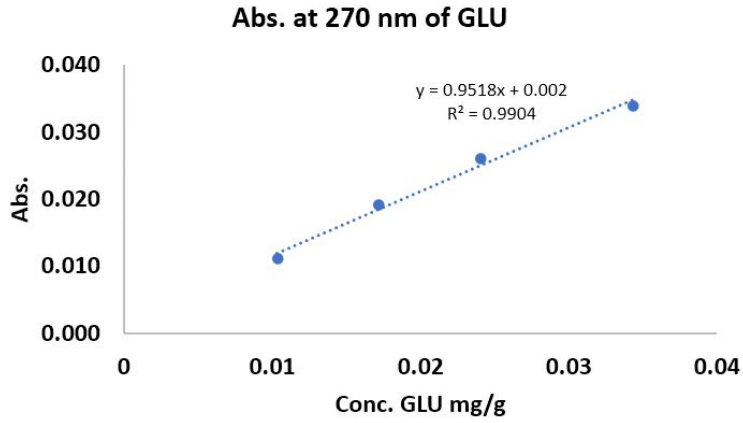

Figure 9 Calibration curve for pure GLU in MeCN at λ= 270 nm.

Please note that although GLU absorbance independently is below the sensitivity of the instrument the effect of GLU on the absorbance of THP in a mixed solution is appreciable. The extent of the influence of GLU is shown in **Table 6** and **Figure 10** for a fixed concentration of THP (0.0058 mg/g) and increasing concentrations of GLU.

Table 6 Concentration of GLU in mg/g in solution with a fixed THP concentration of 0.0058 mg/g.

Mole Fraction ratio of THP: GLU	Conc. GLU mg/g	Abs.
1:0.00	0.000	0.222
1:0.44	0.003	0.227
1:0.87	0.007	0.231
1:1.00	0.008	0.232
1:1.17	0.009	0.233
1:1.31	0.012	0.236
1:2.19	0.017	0.242

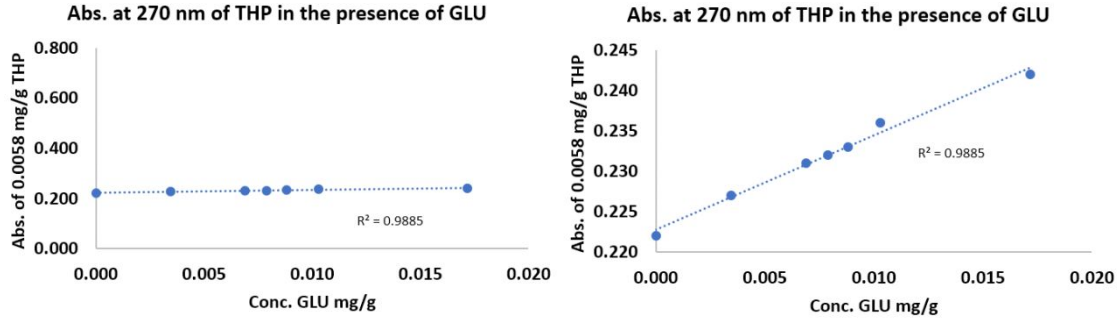

Figure 10 The effect of GLU in solution on the absorbance of a solution with fixed concentration of THP, Table 6. The figure on the right has a zoomed y-axis.

Since there will be different ratios of THP to GLU at eutectic points E1 and E2 the correct calibration curve is needed for analysis of solutions at each composition. The eutectic point E2 is of prime interest, since it is important to establish that the mixed solutions are supersaturated with respect to β-GLU as the nucleating phase. Through a trial and error approach the concentration of THP at the eutectic points E1 and E2 is determined by a calibration curve having the appropriate solution composition.

The calibration curve of THP:GLU 1:1.17 was used for the determination of THP concentration in the presence of GLU for point E2, **Figure 11**, and the values presented in **Table 7**.

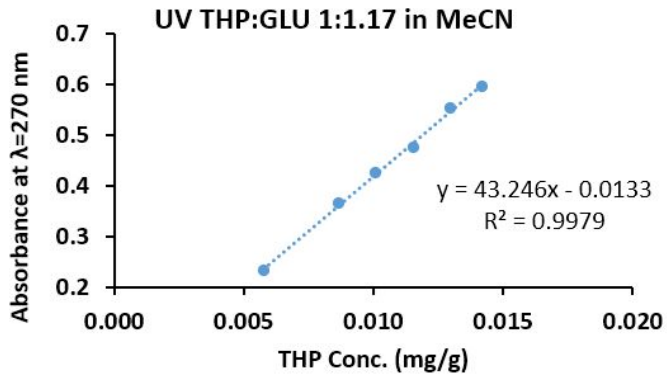

Figure 11 Calibration curve for the absorbance of a 1:1.17 molar ratio solution of THP and GLU.

The calibration curve of THP:GLU 1:0.25 was used for the determination of THP concentration in the presence of GLU for point E1. The calibration curves used for solutions of varying mole fraction ratios of THP to GLU are presented in **Table 7** and plotted in **Figure 12**.

Table 7 Concentration of THP determined from calibration curves of pure THP (1:0), THP in a 1:1 solution 1:1.17 and 1:0.25 solution with GLU.

Pure THP (1:0)		**THP:GLU (1:1)**		**THP:GLU (1:1.17)**		**THP:GLU (1:0.25)**	
Conc. THP mg/g	Abs.	Conc. THP mg/g	Abs.	Conc. THP mg/g	Abs.	Conc. THP mg/g	Abs.
0.0077	0.300	0.00577	0.232	0.00577	0.233	0.00903	0.360
0.0096	0.377	0.00865	0.364	0.01152	0.477	0.00376	0.150
0.0115	0.456	0.01152	0.489	0.00865	0.365		
0.0134	0.533	0.01296	0.541	0.01009	0.426		
0.0154	0.599	0.01440	0.611	0.01296	0.555		
				0.01419	0.596		

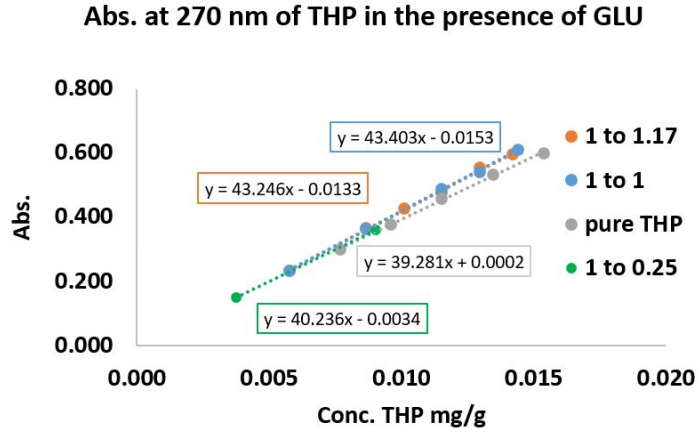

Figure 12 Calibration curves for the absorbance of THP created as per Table 7.

Samples E1 B3 and E2 B3 were diluted appropriately and the absorbance values obtained at 270 nm. The concentration in mg/g of THP in these samples was extracted from the respective calibration curves, **Figure 12** and **Figure 11**. The concentration of the samples are calculated

prior to dilution and are displayed in **Table 8** along with the calculated mass of THP in the original samples.

Table 8 Absorbance and concentration of THP in MeCN of samples E1 B3 from 1:0 calibration curve and E2 B3 from 1:1.17 calibration curve. The concentration of THP in the samples before dilution. The mass of MeCN added to dissolve the solid from the samples for UV-analysis. The total mass accounted for by THP in the original samples and the weight of the total solid (THP + GLU) from the dried samples and thus the mass of GLU.

	absorbance	THP mg/g*	Conc. THP before dilution (mg/g)	Mass of MeCN (g)	Mass of THP (g) (conc. x g of MeCN)	Total solid (g)	Mass of GLU (g)
E1 B3	0.360	0.00903	0.90315	73.74653	0.06660	0.07874	0.01214
E2 B3	0.243	0.00531	0.25632	73.84660	0.01961	0.03661	0.01700

* – mg solute /g solvent

The corresponding ternary coordinates in mole fraction are shown in **Table 9** and the eutectic points are shown on the TPD in Figure 16 of the manuscript**.**

Table 9 The mole fraction (MF) compositions of the liquid phase in equilibrium at the eutectic points E1 and E2 from respective calibration curves of 1:0.25 for point E1 and 1:1.17 for point E2.

	Mass of CLO (g)	Moles THP	Moles GLU	Moles CLO	THP MF	GLU MF	CLO MF
E1 B3	29.0686	3.69E-04	0.92E-04	0.24352	**0.00152**	**0.00038**	**0.99810**
E2 B3	29.1017	1.09E-04	1.29E-04	0.24379	**0.00045**	**0.00053**	**0.99903**

20 mL induction time experiments

Table 10 Amount of solid (g) added to solvent (CLO) (g) for desired mole fraction concentration (MF) and supersaturation (S) when T_{nuc}=10°C for induction time experiments.

Solid (g)	Solvent (g)	MF conc. Saturated ($x10^3$)	MF conc. equilibrium ($x10^3$)	S
GLU				**X/X^***
0.4125	744	0.50	0.21	2.43
0.3960	744	0.48	0.21	2.34
0.3795	744	0.46	0.21	2.24
0.3300	744	0.44	0.21	1.95
0.3000	744	0.40	0.21	1.77
0.2500	744	0.30	0.21	1.47
0.2300	744	0.27	0.21	1.36
0.2100	744	0.25	0.21	1.24
0.2000	744	0.24	0.21	1.18
THP:GLU				**$(X^{AB})^2/(X^{AB*})^2$**
1.9000	350	2.07	0.55	13.97
3.7200	744	1.90	0.55	11.86
3.5000	744	1.79	0.55	10.50
3.3300	744	1.70	0.55	9.51
3.1000	744	1.59	0.55	8.24
2.9770	744	1.52	0.55	7.60
2.9200	744	1.49	0.55	7.31
2.9000	744	1.48	0.55	7.21
2.8800	744	1.47	0.55	7.11
2.8600	744	1.46	0.55	7.02
2.8520	744	1.46	0.55	6.98

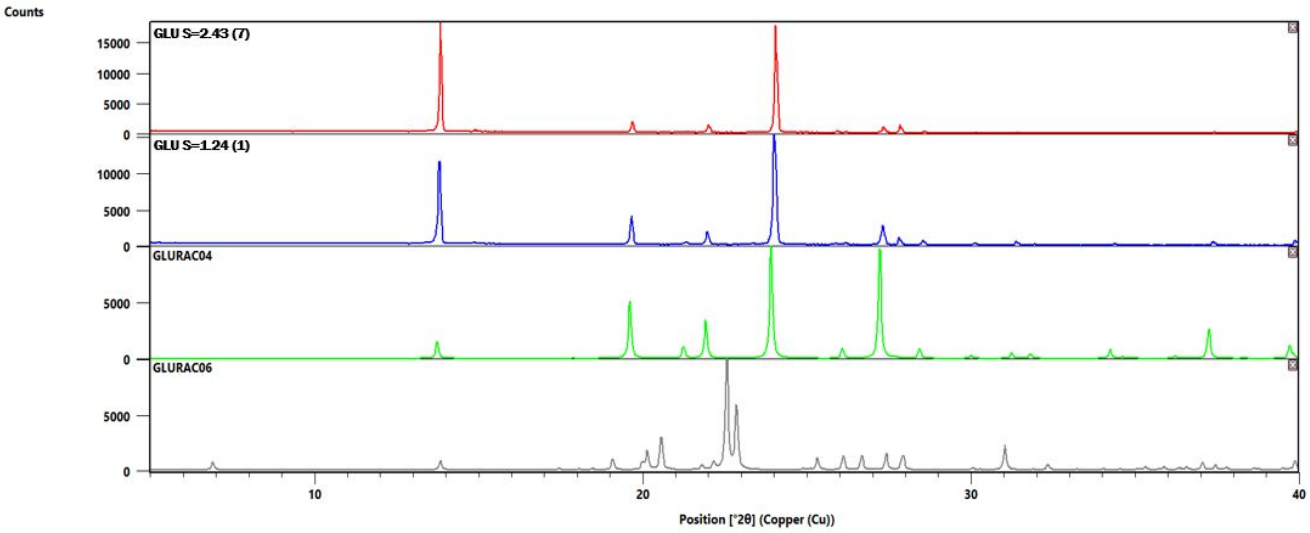

Figure 13 Nucleating solid in pure GLU is β-glutaric acid CSD ref. code GLURAC04. α-glutaric acid is also shown CSD ref. code GLURAC06.

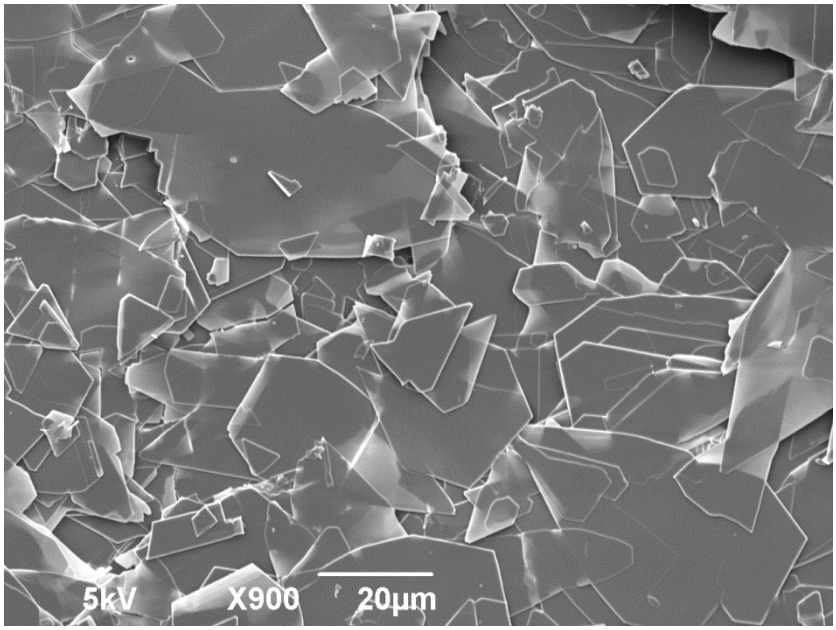

Figure 14 THP II nucleated in chloroform at 10 °C.

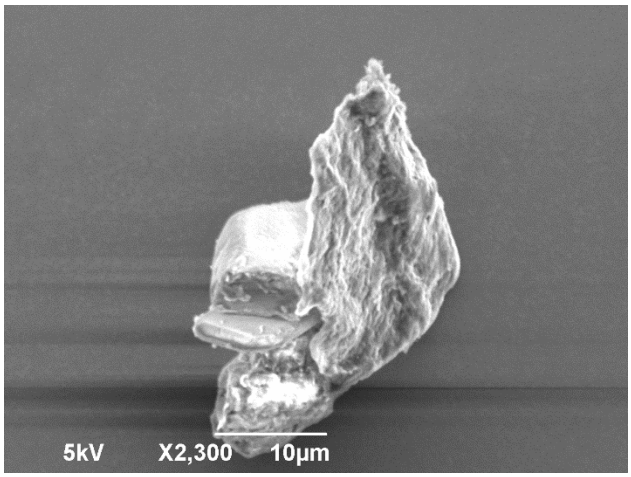

Figure 15 β-GLU nucleated in chloroform at 10 °C.

Nucleation is detected visually as the solution becomes slightly cloudy with fine solid particles dispersed. After some time (about 20 minutes depending on driving force) there is a further increase in turbidity. The solid begins sticking/adhering to the vials from 7 up to 20 minutes post nucleation depending on driving force. SEM micrographs taken of solid isolated from induction time experiments after 120 hours, reveal the adhering samples consists of larger crystals, **Figure 17**, amongst small hexagonal blocks and the samples which remained suspended as just small diamond shaped blocks, all of which resemble THP:GLU cocrystals. PXRD diffractograms **Figure 16** of both samples revealed diffractograms corresponding to pure THP:GLU cocrystal. Even when cocrystals are added as seeds to CLO the crystals aggregate and adhere to the glass surface of the vial near the liquid surface. A solid phase attaching to the glass surface is a strong indication of cocrystal, however admittedly the cocrystal didn't always attach early to the glass.

Table 11 S=13.97 batch report

Vial no.	Time Nucleated	Time Filtered	State	PXRD
5	00:07:20	00:09:40	Disp.	CC
3	00:07:48	00:10:00	Disp.	CC
2	00:07:58	00:15:10	Disp. w/ sticky ring	CC
1	00:08:16	00:17:22	Disp. w/ sticky ring	CC
9	00:08:31	02:19:37	Sticking but some disp.	CC
7	00:08:56			
10	00:07:30	03:50:15	Sticking	CC
4	00:11:15	02:13:55	Sticking	CC
6	00:13:56	120 hr	V. Turbid disp.	CC
8	00:14:00	120 hr	Sticking	CC

Disp. (dispersed) means that at time of filtering the solid was totally in suspension and there is a slight turbidity observed by eye. Disp. with sticky ring describes how the solid is mainly dispersed however there is slight aggregation of solid beginning to stick to the glass appearing as a ring around the glass towards the bottom of the vial. Sticking with some dispersed solid describes an intermediate state where solid is deposited on the walls however some solid remains in suspension. Sticking describes that all solid is fixed to the glass walls. Vial number 6 as seen was very turbid and never evolved to the totally sticking state.

All vials from S=13.97 batch were filtered and examined by PXRD. In some cases PXRD peaks are present for both β-GLU and THP:GLU cocrystal as can be seen in **Figure 16** for the S=13.97 batch. Vial 1 and vial 2 were filtered 9 and 6 minutes after the first detection of nucleation respectively.

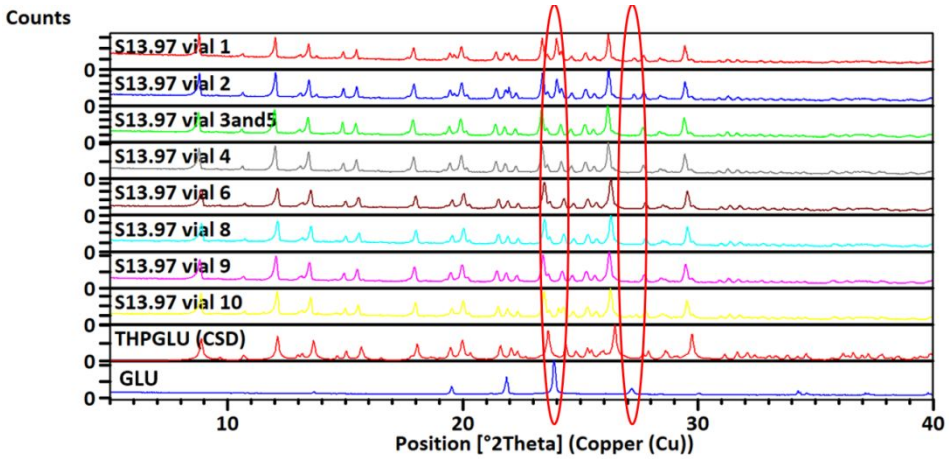

Figure 16 Diffractograms obtained for solid residues from S=13.97 induction time experiments batch at 20 mL scale. Peaks common to β-GLU are highlighted in vial 1 and 2.

Figure 17 and **Figure 18** show that the suspended crystals are small hexagonal blocks closely resembling THP:GLU cocrystals, whereas the adhering sample consists of larger crystals

amongst similar small hexagonal blocks. PXRDs of both samples revealed diffractograms corresponding to pure THP:GLU cocrystal.

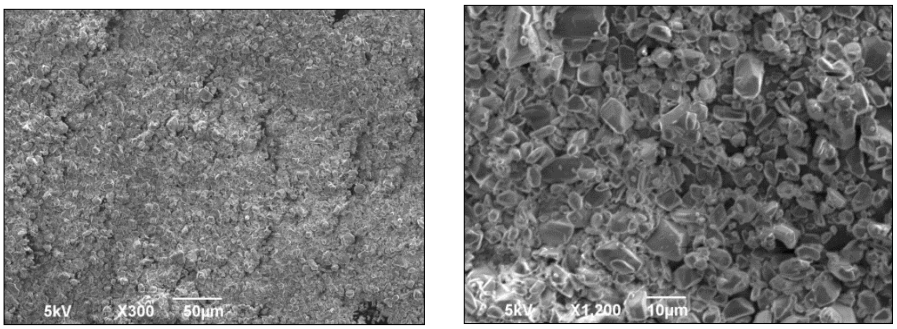

Figure 17 S=13.97 vial no. 6 filtered after 120 hr at T_{nuc} where the solid phase remained in suspension.

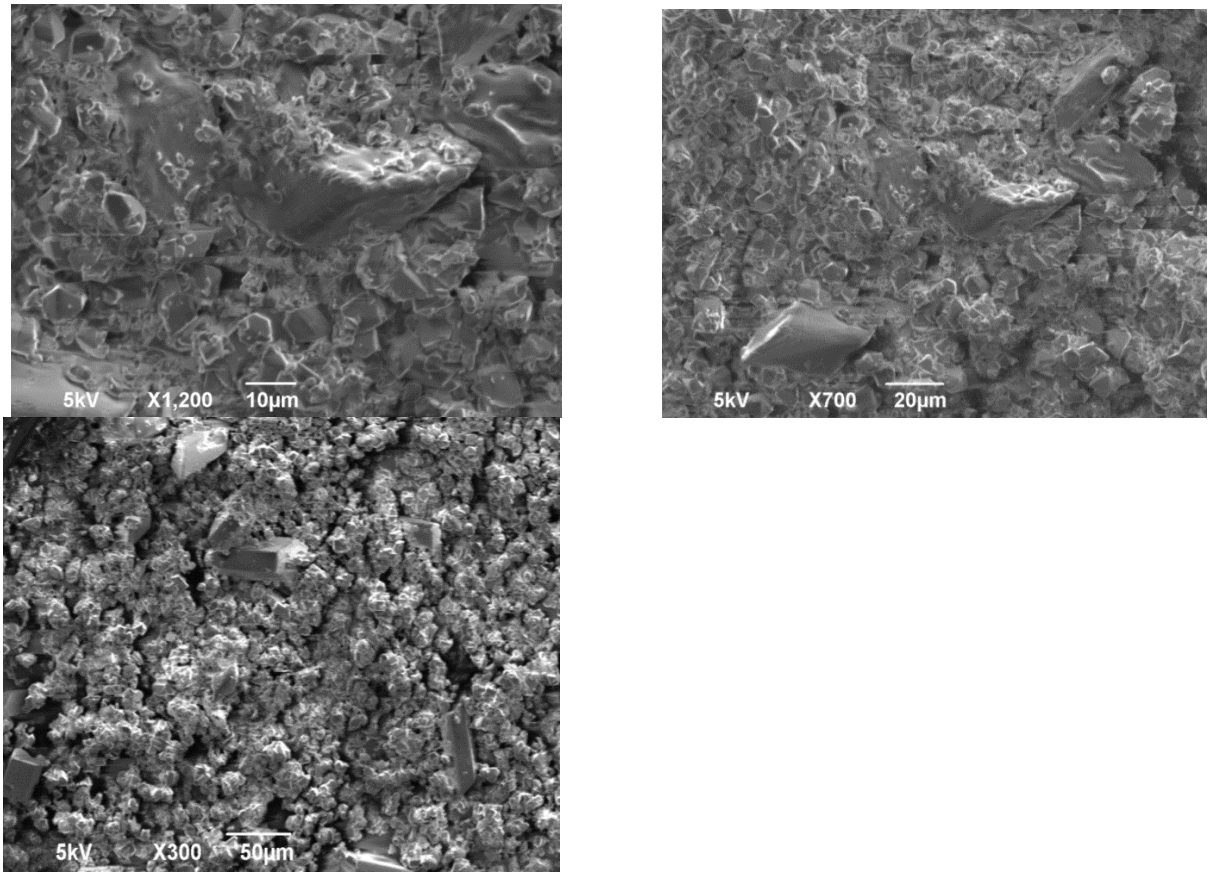

Figure 18 S=13.97 vial 8 filtered after 120 hr at T_{nuc} where the solid phase was completely adhered to the sides of the glass vial.

An SEM of a sample from the S=7.21 batch (**Figure 19**) exhibits larger crystals similar to those seen in **Figure 18** and the powder pattern showed pure THP:GLU cocrystal suggesting that the large crystals in **Figure 17** and **Figure 18** are cocrystals that have grown.

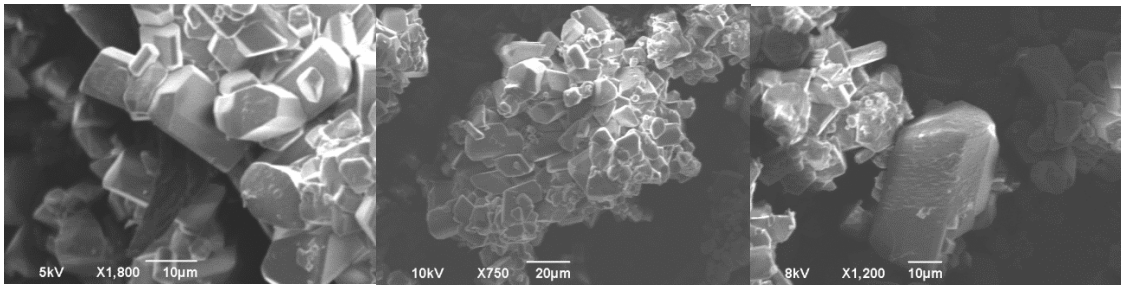

Figure 19 S=7.21 vial 19 filtered after 72 hr at T_{nuc} where all solid was adhering to the sides of the glass vial.

Samples were also taken of the S=7.21 batch. Considering the small amount of solid appearing in the vials initially, samples of vials nucleating at the same time were combined in order to have enough solid sample to test. The patterns from S=7.21 batch match that of the cocrystal. Sample vial 7-11 is of poor quality due to sample preparation.

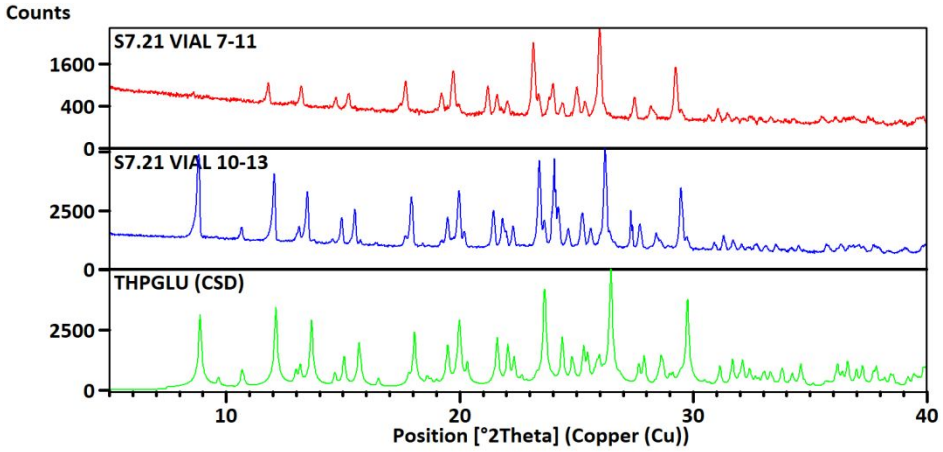

Figure 20 Diffractogram of solids isolated in dispersed state from S=7.21 batch.

The solids from S=9.51 vials 19, 14 and 1 all nucleated at the same time and were filtered together to isolate enough solid for the PXRD. They were filtered 2 minutes after the first appearance of crystals in solution which seems to be enough time for the solid to be cocrystal. Vials 9 and 15 from the same batch were filtered at a later stage when solid began to stick to the sides of the vial but the bulk was still in suspension. The solid isolated in the two vials at this stage seems to be pure cocrystal as seen from the diffractograms in **Figure 21** .

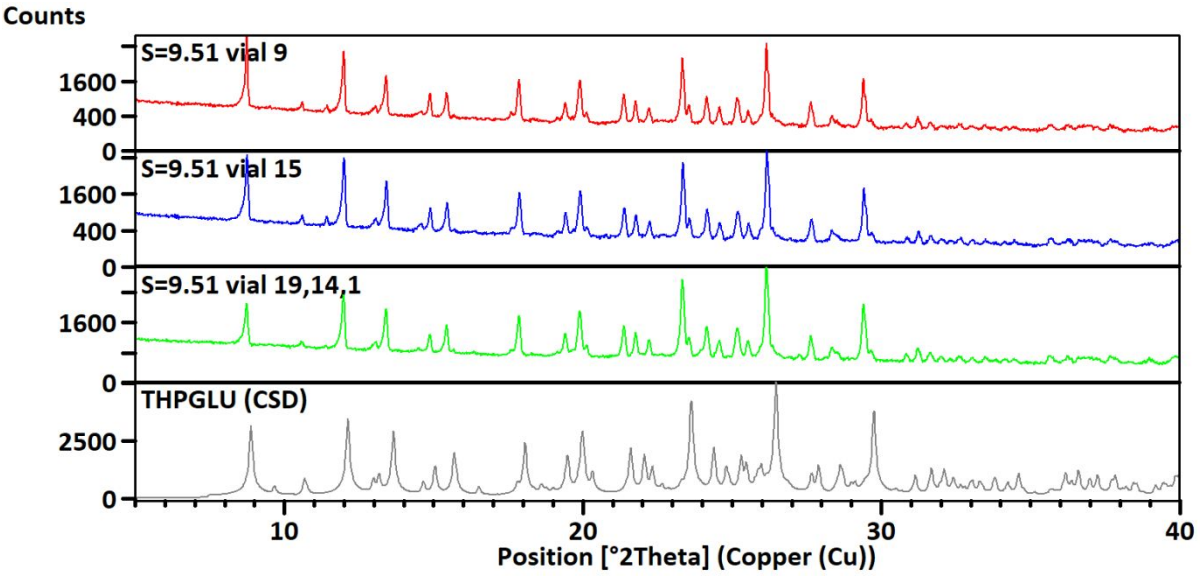

Figure 21 PXRD Filtrates from S=9.51 batch at various time points following nucleation show pure cocrystal.

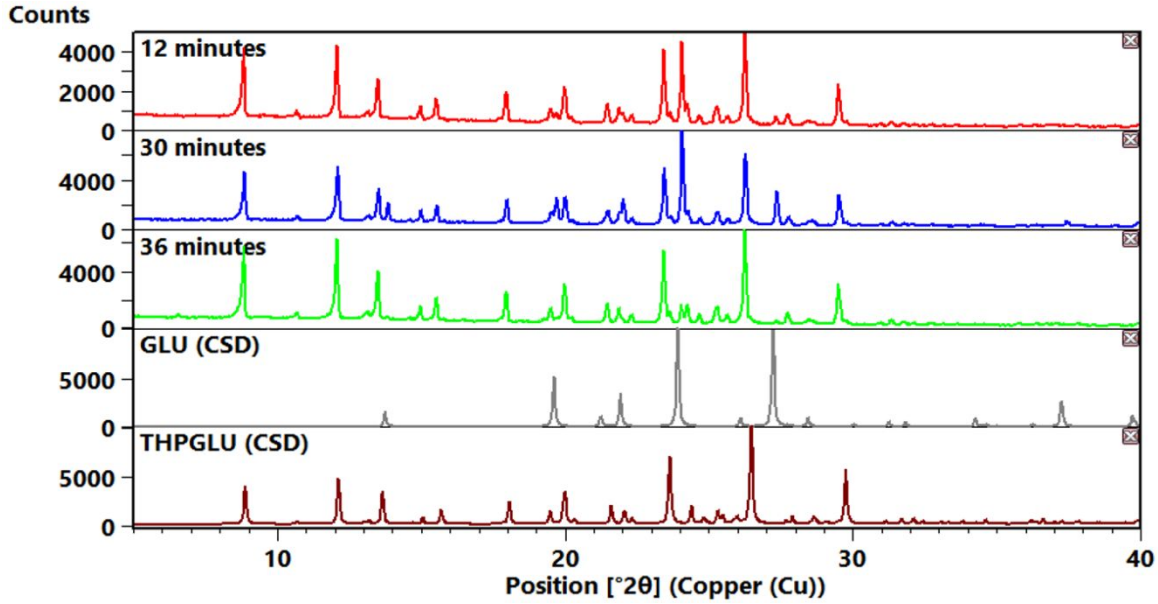

Figure 22 Diffractograms obtained for solid residues from S=8.24 samples filtered 12, 30 and 36 minutes post nucleation with peaks corresponding to both THP:GLU and β-GLU.

The sample IDs in **Table 12** are labelled to describe their visual state at the time of filtration with 'd' meaning dispersed, 'm' meaning a mixture of solid dispersed and adhering to vial surfaces and 'H' means the solid was totally adhered.

Table 12 Samples filtered from S=8.24 batch.

S=8.24			
Sample ID	**Nucleated**	**Filtered**	**Time elapsed**
2H	0:19:00	1:27:00	1:08:00
1d	0:20:00	0:32:00	0:12:00
19m	0:16:05	0:46:05	0:30:00

20m	1:02:00	1:32:40	0:30:40
9H	0:52:55	1:29:45	0:36:50
10m	0:57:00	3:40:00	2:43:00
12H	1:35:40	2:12:00	0:36:20
13H	1:36:30	3:42:00	2:05:30

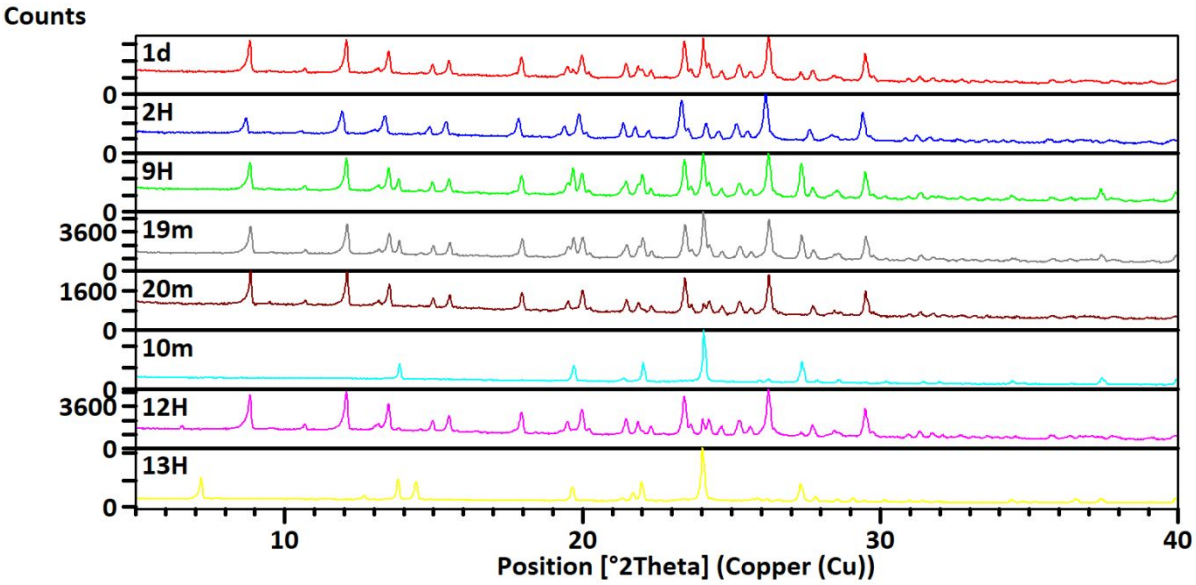

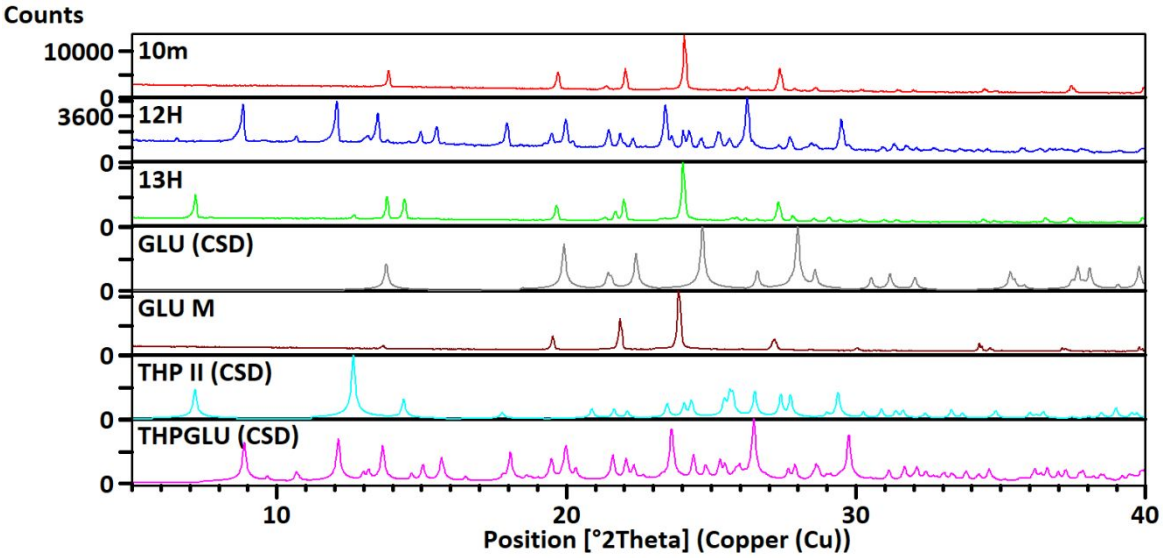

Figure 23 PXRD of filtrates from S=8.24 at different stages. 'd' notates that the solid is in the dispersed phase, 'H' means that the solid is present heterogeneously sticking to the sides of the vial and 'm' means that the solid is a mixture of sticking to the sides and some solid remains in suspension.

Upon examination of the above diffractograms it appears that vial 10 consists of β-GLU, 12 is almost identical to pure THP:GLU. Vial 13 is a mixture of β-GLU with some extra peaks seen in the THP:GLU cocrystal pattern.

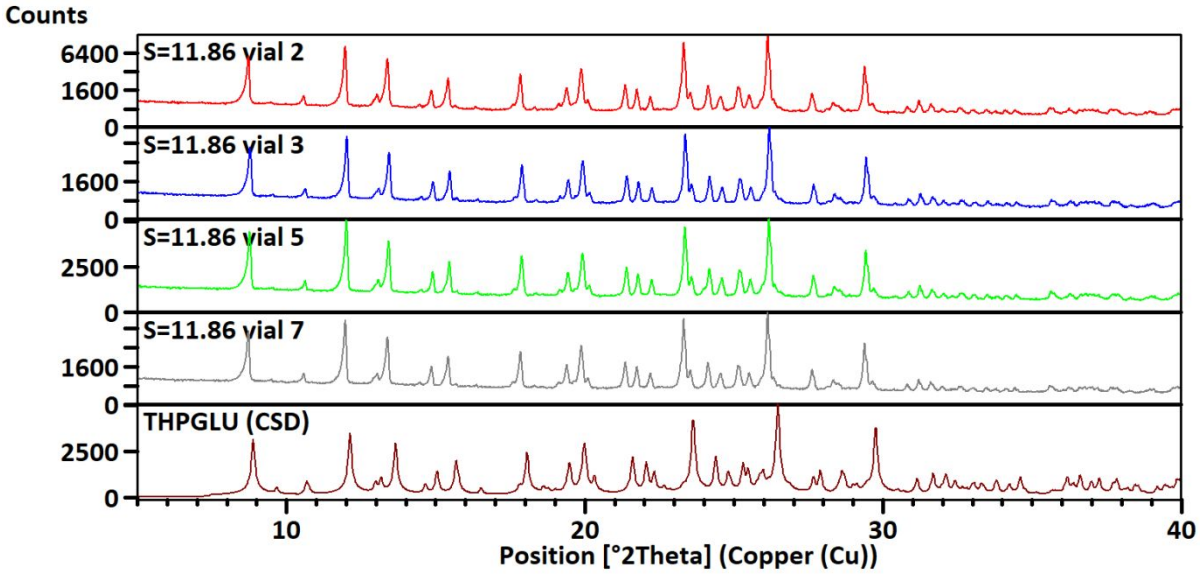

248

249 **Figure 24 All solid filtered from S=11.86 batch after 24 hours is pure cocrystal.**

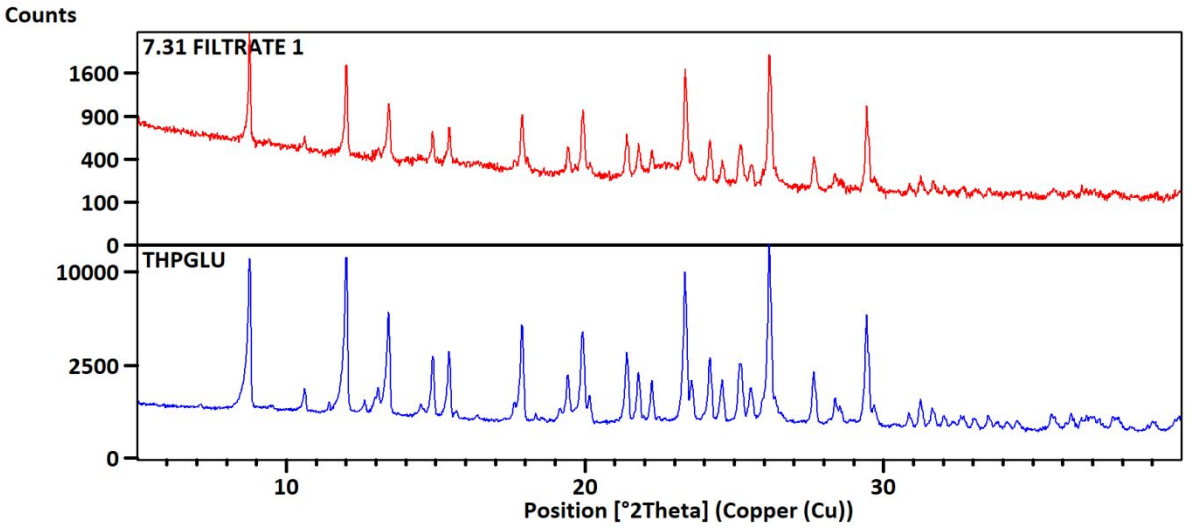

250

251 **Figure 25 Vial 1 from S=7.31 batch was filtered in the dispersed state 2 minutes after the**
252 **first detection of nucleation. The pattern matches that of pure cocrystal.**

253

SEMs from S=7.11 batch

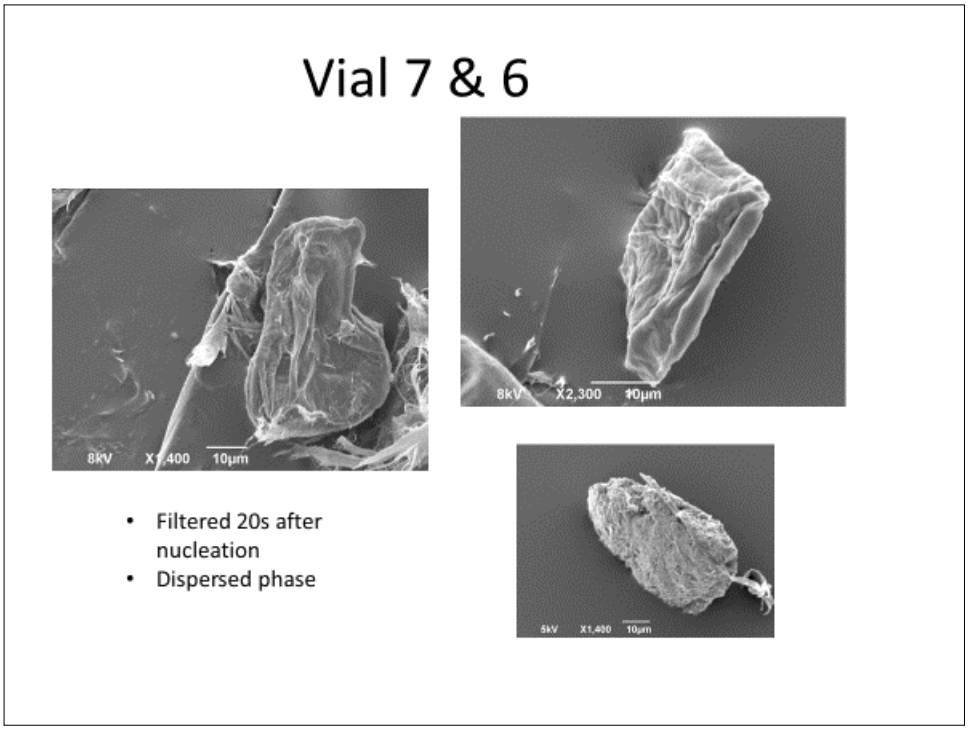

Figure 26

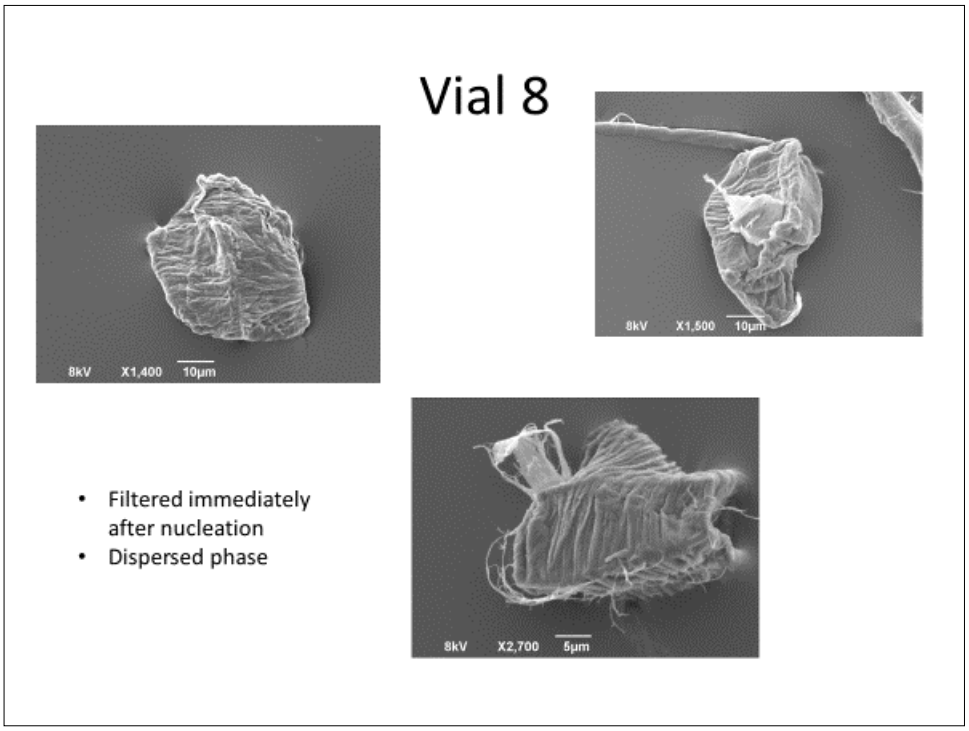

Figure 27

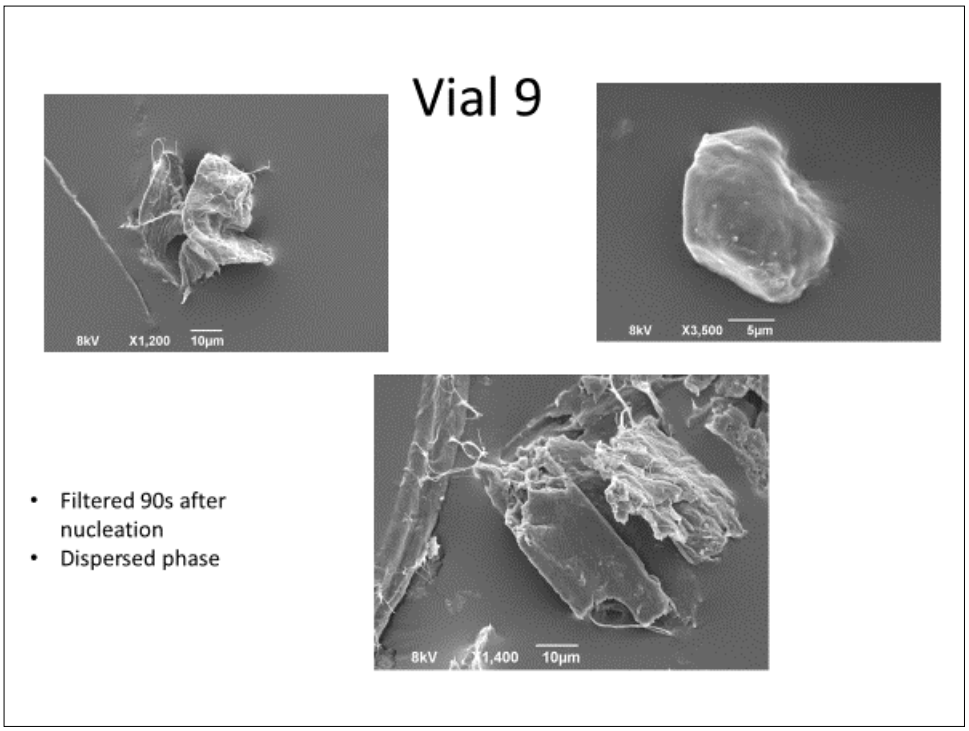

259

260 **Figure 28**

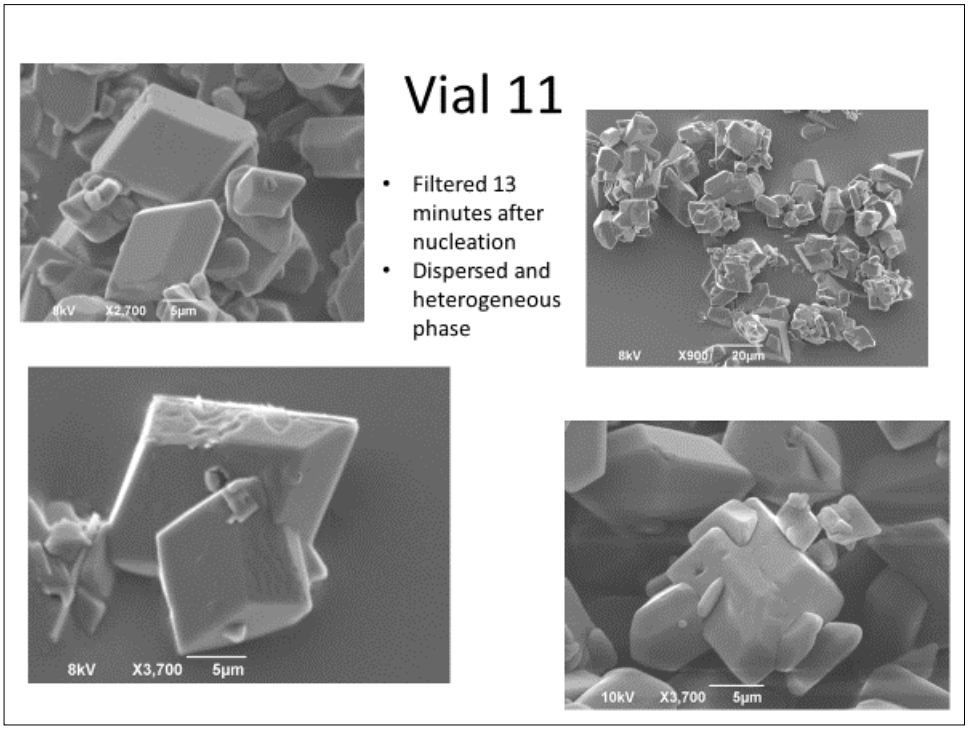

261

262 **Figure 29**

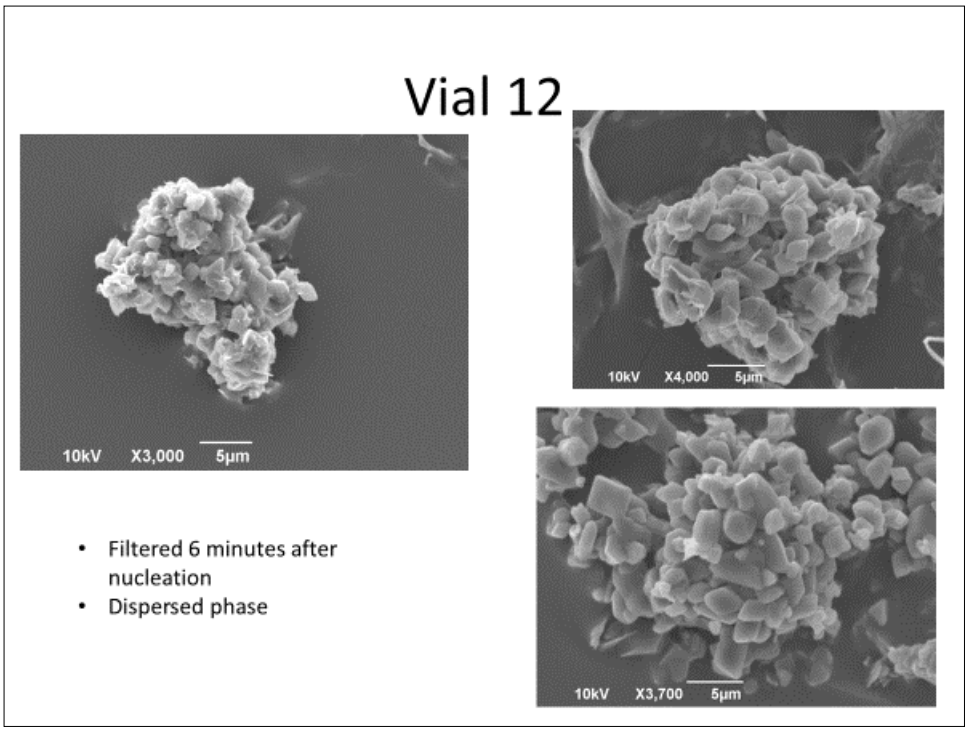

Figure 30

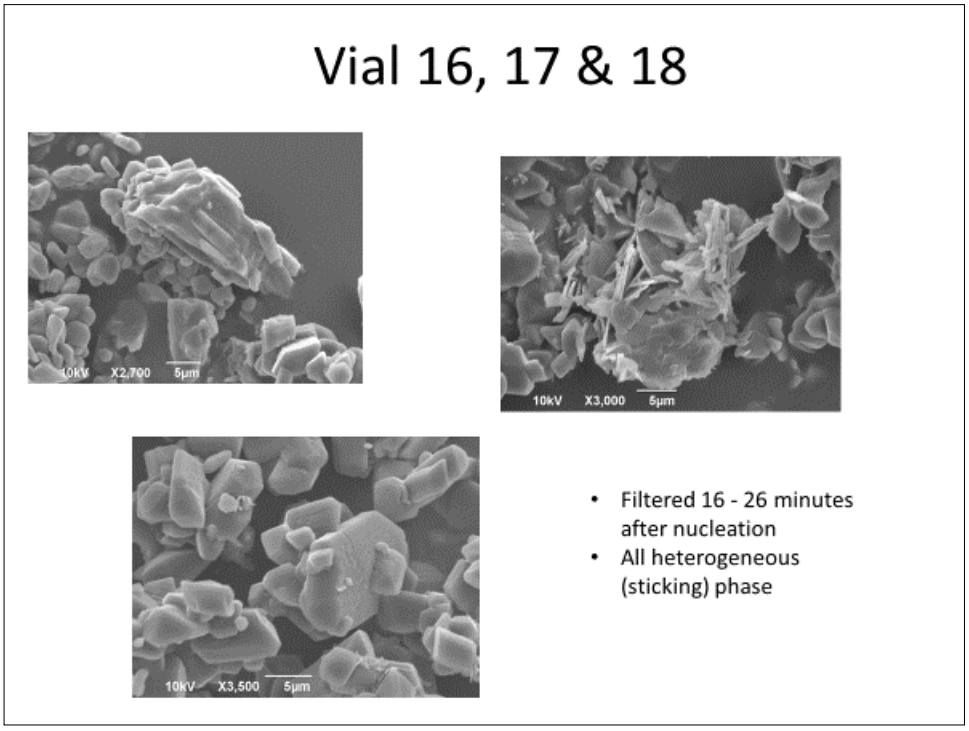

Figure 31

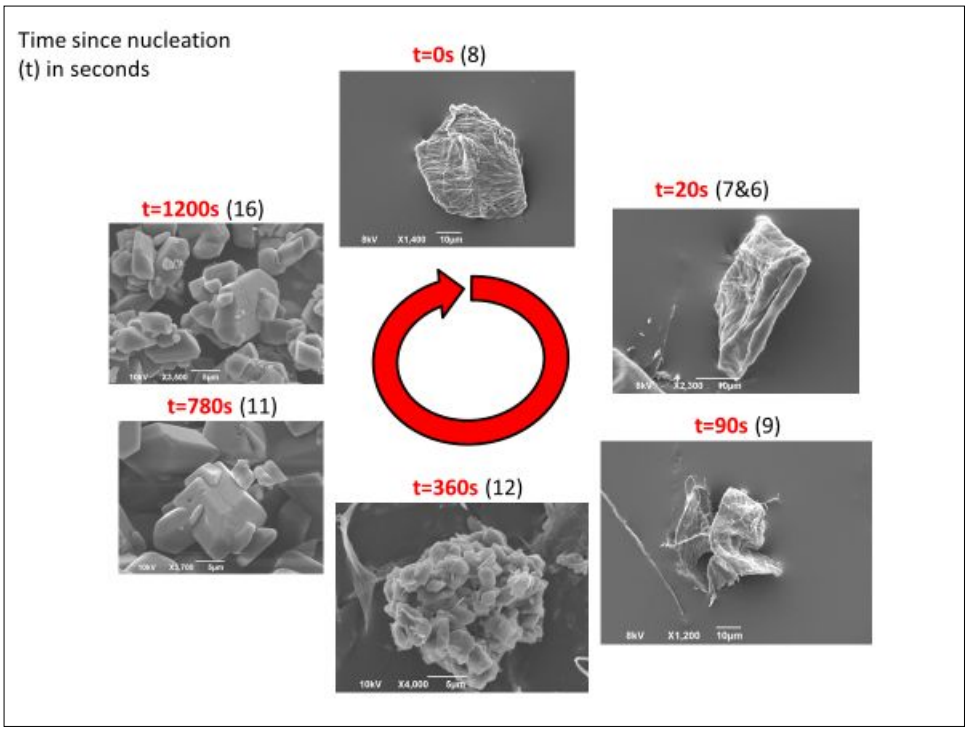
Time since nucleation
(t) in seconds
t=0s (8)
t=20s (7&6)
t=1200s (16)
t=780s (11)
t=90s (9)
t=360s (12)

Figure 32

250 mL experiments in Optimax

Experiment A

In experiment A, a decrease in intensity of the THP peak was observed by ATR-FTIR at time 1:07:26 signifying the uptake of THP from solution into a solid phase (**Figure 33 (a)**). Unexpectedly, the solution concentration of THP begins to increase again at time 1:55:00 as a result of crystals adhering to the probes and surfaces in the reactor, leading to unreliable results beyond this point. This correlates with a sudden noticeable increase in the FBRM reading at this time also, however, the spike in particle counts around the 2 hour time point is not a result of primary nucleation, it is due to the solid beginning to stick to the probe. At a higher resolution, **Figure 33 (c),** it is obvious that primary nucleation occurs much earlier with an increase in particle counts identified by FBRM at time 1:04:07 revealing the onset of nucleation.

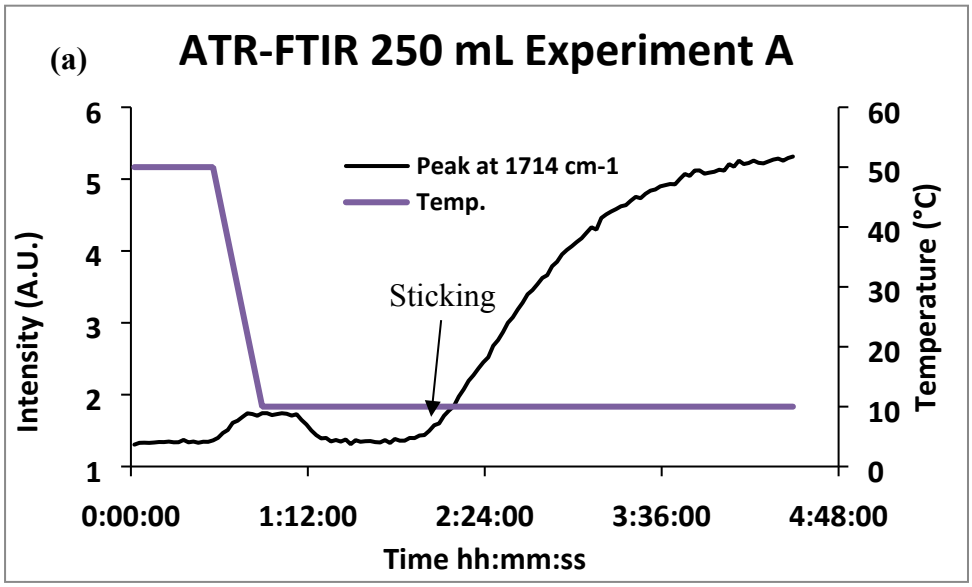

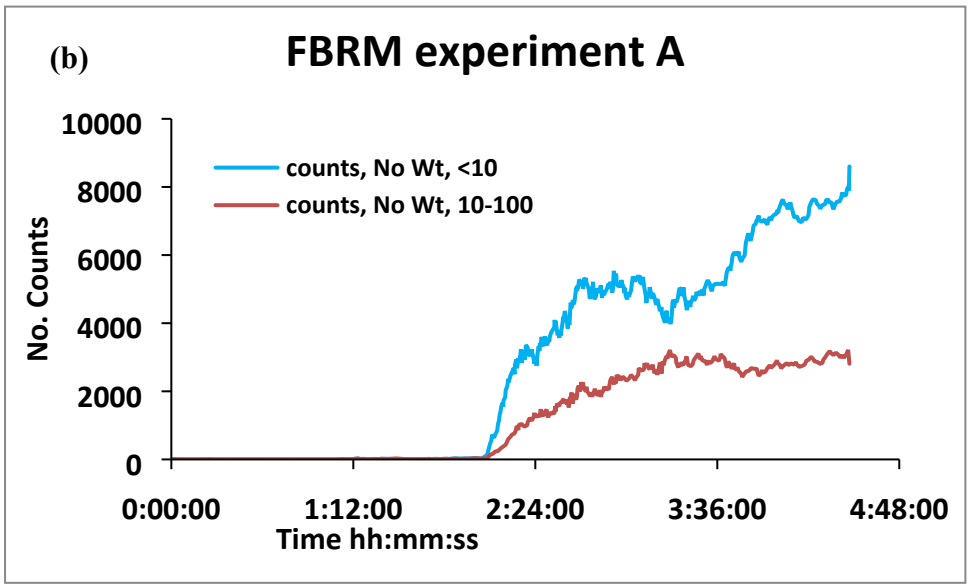

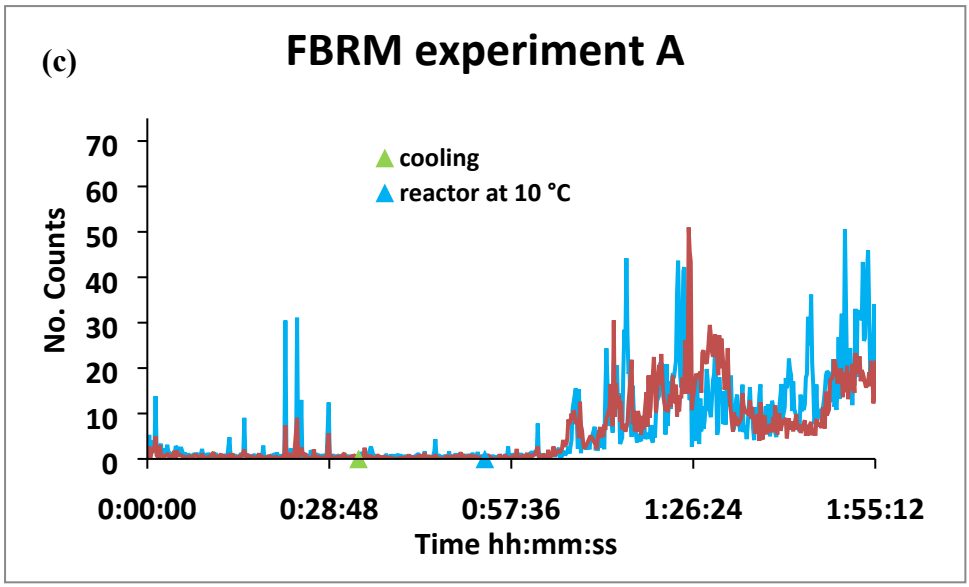

Figure 33 (a) shows ATR-FTIR spectrum from experiment. (b) shows the FBRM particle counts from experiment A. (c) is a zoomed image into the nucleation region of the FBRM graph.

Experiment B

In experiment B two 10 mL samples were taken at different time points and filtered. The isolated solid was analysed by PXRD and SEM. A decrease in the THP 1714 cm^{-1} peak intensity was observed at time 0:51:26, **Figure 34 (a)**. Particles were detected by FBRM at time 0:47:17 which is 4 minutes before THP concentration decrease was detected (**Figure 34 (c)**). The first sample (Sample 1B) was taken when a decrease in the solution concentration of THP was observed by ATR-FTIR at time 1:11:26. The second sample (Sample 2B) was taken a time 2:03:26 to investigate transformation of the solid phase.

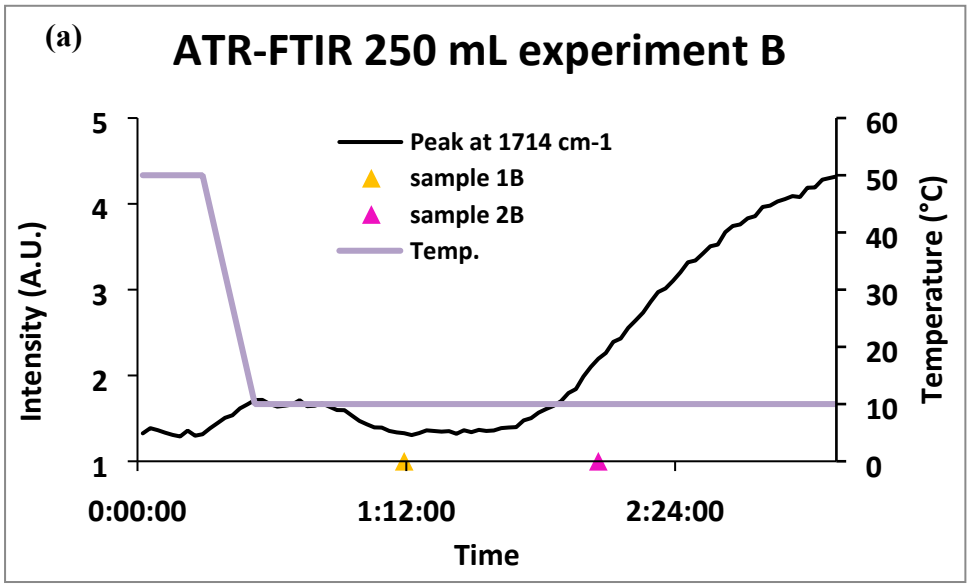

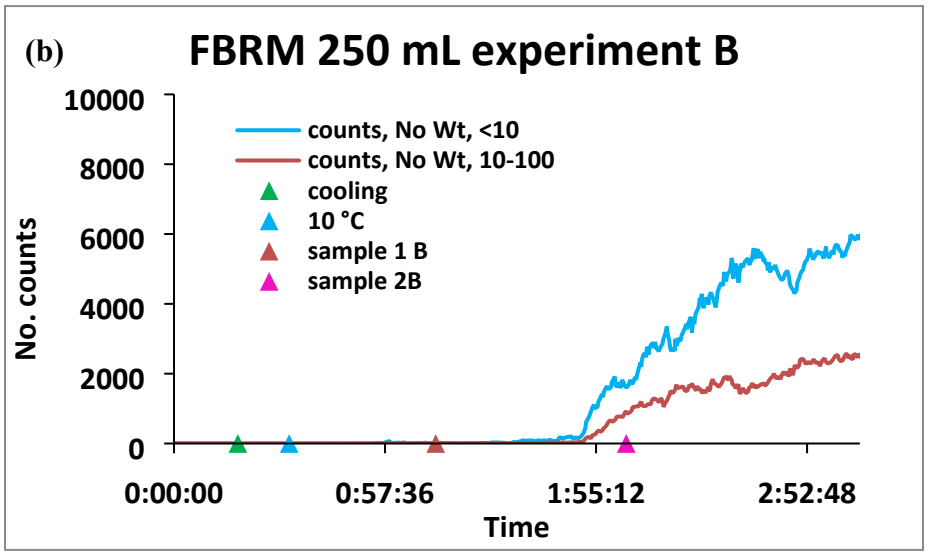

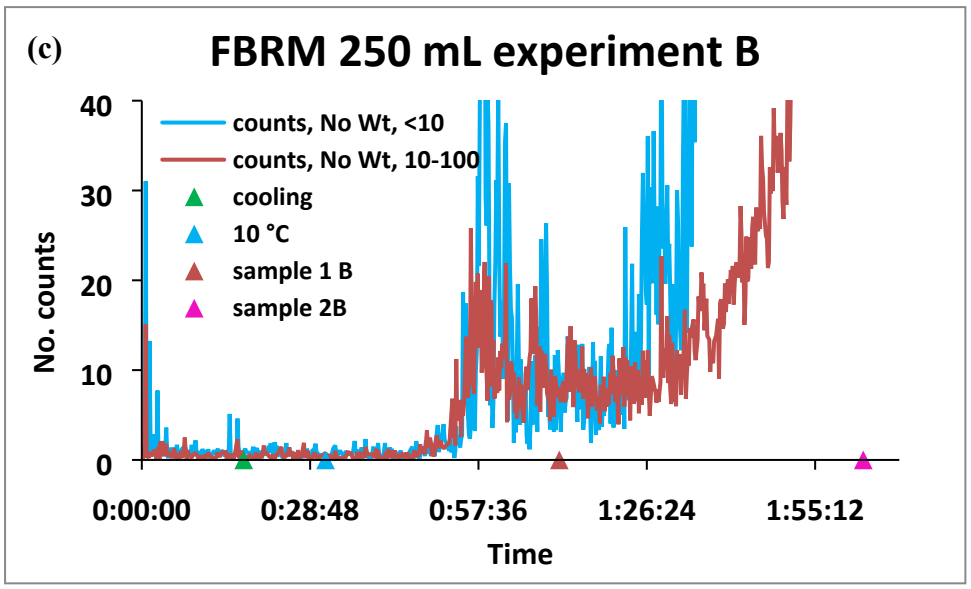

Figure 34 (a) ATR-FTIR spectrum from experiment B with symbols indicating sample points. (b) FBRM particle counts from experiment B. (c) A zoomed image of the FBRM graph to observe the early stages of particle detection.

PXRDs of samples 1B and 2B presented very different diffractograms (**Figure 35)** wherein Sample 1B in closely resembles the pattern of β-glutaric acid (GLU (CSD)).

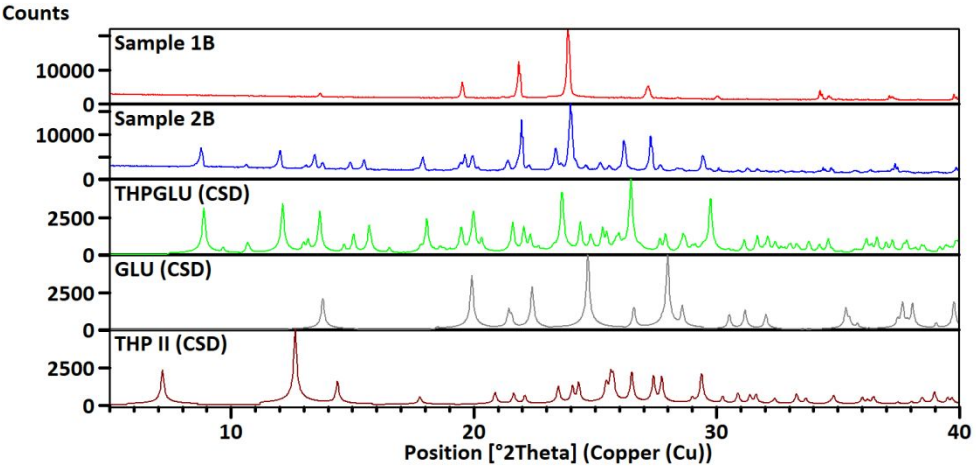

Figure 35 PXRD of samples 1B and 2B versus cocrystal and pure components.

All peaks for Sample 1B are common to β-GLU however, there are some extra peaks from the β-GLU (CSD. Ref. code GLURAC04) pattern that are not present in Sample 1B. Sample 1B could represent a new GLU form or the crystals obtained were not of sufficient quality to observe all of the peaks. The pattern does not match any known polymorphs of glutaric acid but is closest to the β-glutaric acid form and it is most likely that missing peaks are due to resolution and sample quality and that the sample is pure β-GLU.

A PXRD of Sample 2B (**Figure 36**) shows a diffractogram close to that of the pure THP:GLU cocrystal.

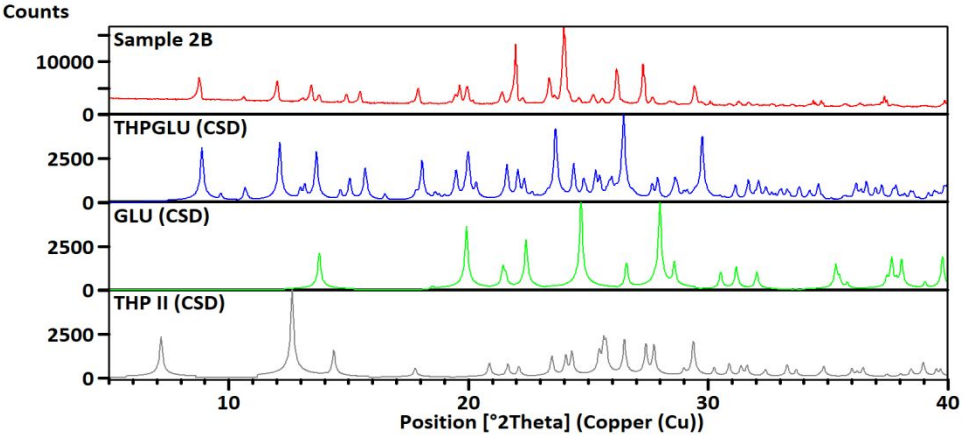

Figure 36 PXRD pattern for sample 2B.

Peaks corresponding to both THP:GLU cocrystal and β-GLU are present in the PXRD pattern of sample 2B (**Figure 36** and **Figure 35**) suggesting that sample 2B is a mixture of THP:GLU cocrystal and GLU.

SEM images in **Figure 37** and **Figure 38** reveal a visible difference in the appearance of crystals from sample 1B versus 2B. Sample 1B solid appears as jagged shard-like crystals as seen in **Figure 37**.

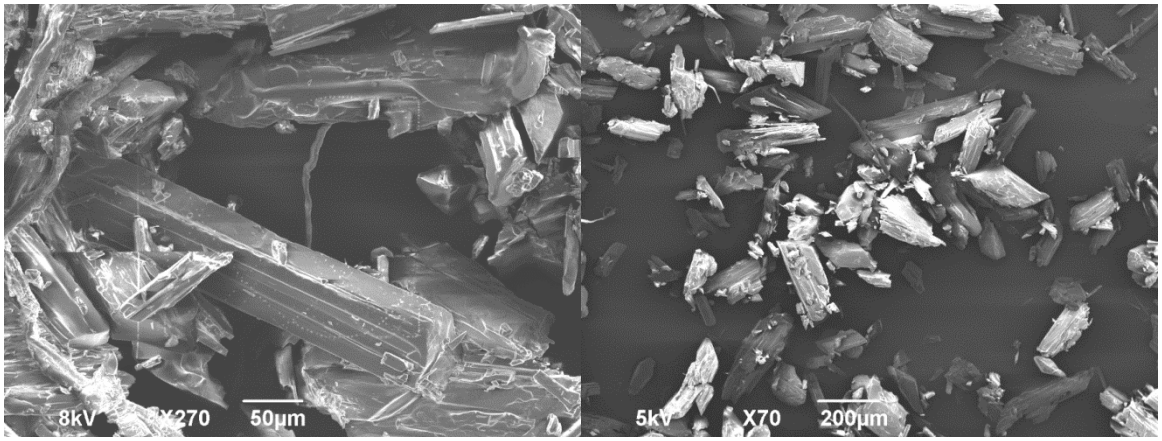

Figure 37 SEM images of sample 1B at different magnifications (a) x70 and (b) x270.

SEM images of sample 2B in **Figure 38** show the shard-like crystals from sample 1B covered in smaller hexagonal block crystals similar to THP:GLU cocrystal. It is postulated that THP:GLU cocrystals are formed through secondary nucleation on β-GLU templates and proceed to grow as the metastable β-GLU dissolves, similar to solution mediated phase transformation (SMPT) of metastable polymorphs to more stable forms.[1]

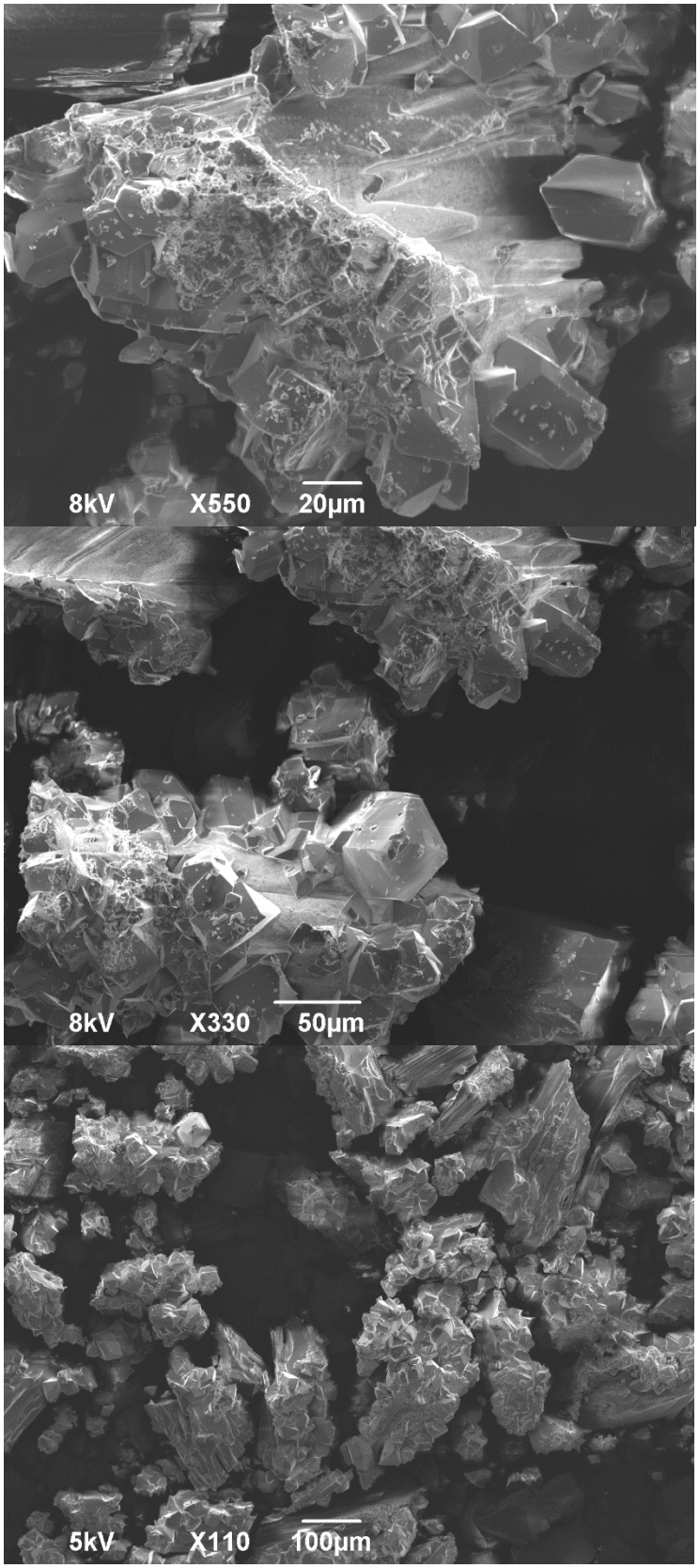

Figure 38 SEM images of sample 2B at different magnifications.

The hexagonal blocks that appear in the SEM of sample 2B appear to be THP:GLU cocrystal as previously discovered.[2]

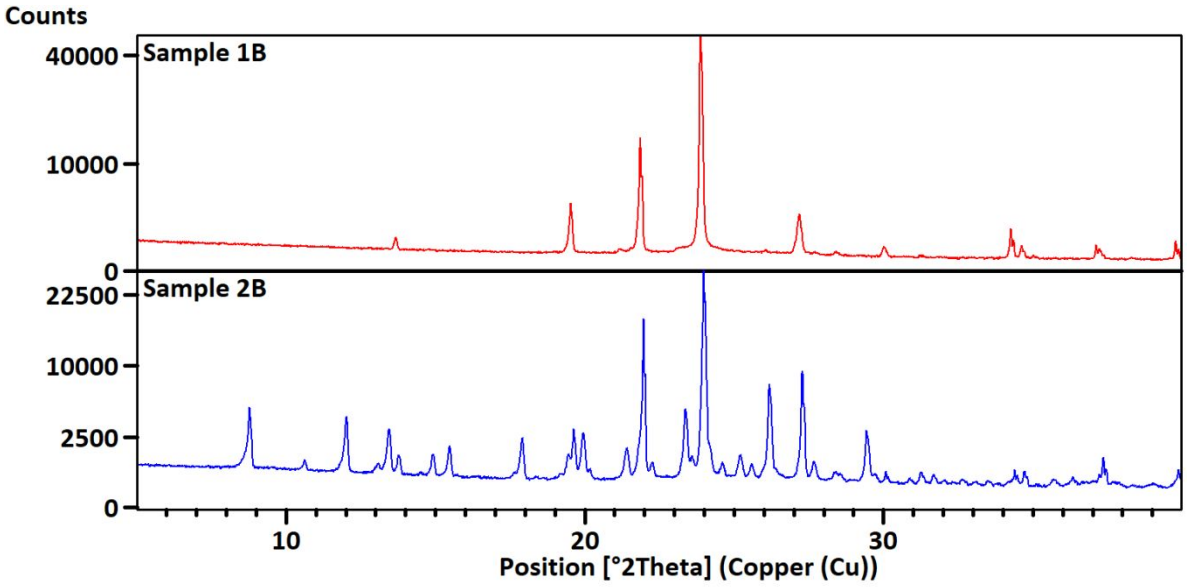

Figure 39 PXRD of sample 1B versus 2B.

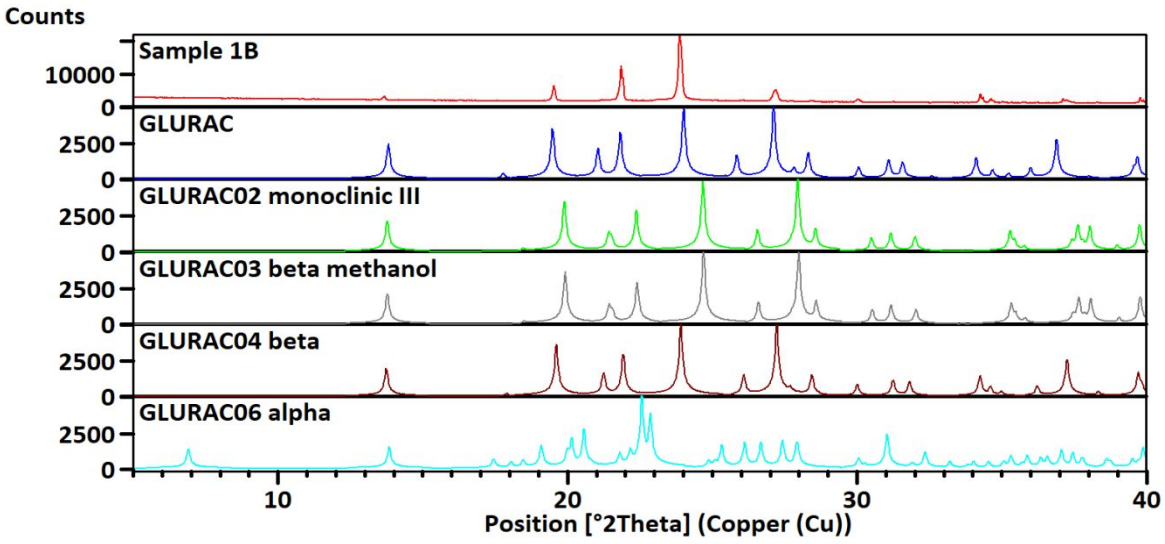

Figure 40 PXRD of Sample 1B versus all known polymorphs of glutaric acid from the CSD.

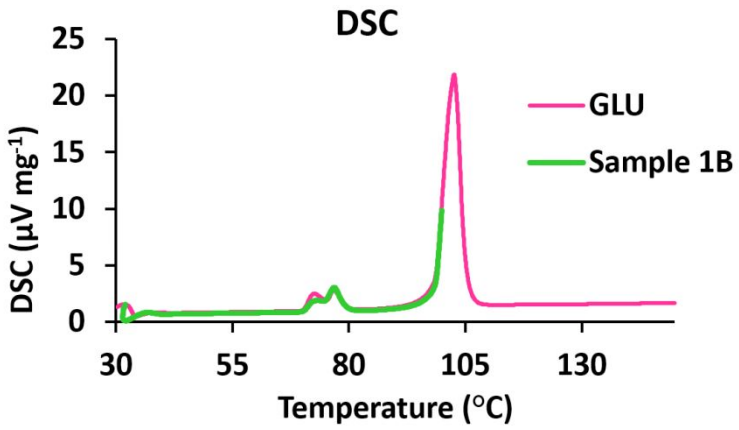

Figure 41 DSC of Sample 1B shows endotherms characteristic of β-glutaric acid (GLU) with endotherm peak at 97 °C for the α-polymorph with a transition from β to α at 74 °C. The sample DSC measurement stopped at 100 °C.

Experiment C

Table 13 Samples taken during 250 mL experiment C. The 'time' refers to time passed since recording of experiment is initiated on ATR-FTIR and FBRM probes.

Sample number	Time (h:mm:ss)
1C	1:07:00
2C	1:10:00
3C	1:21:00
4C	1:30:00
5C	1:42:00
6C	1:52:00
7C	2:05:00
8C	2:31:00
9C	2:55:00

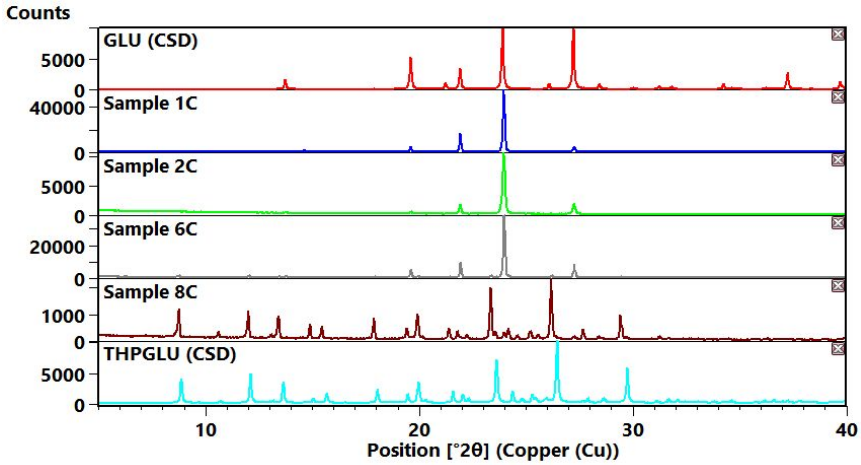

Figure 42 PXRD of samples from experiment C demonstrates the transformation of the β-GLU phase to pure cocrystal.

361

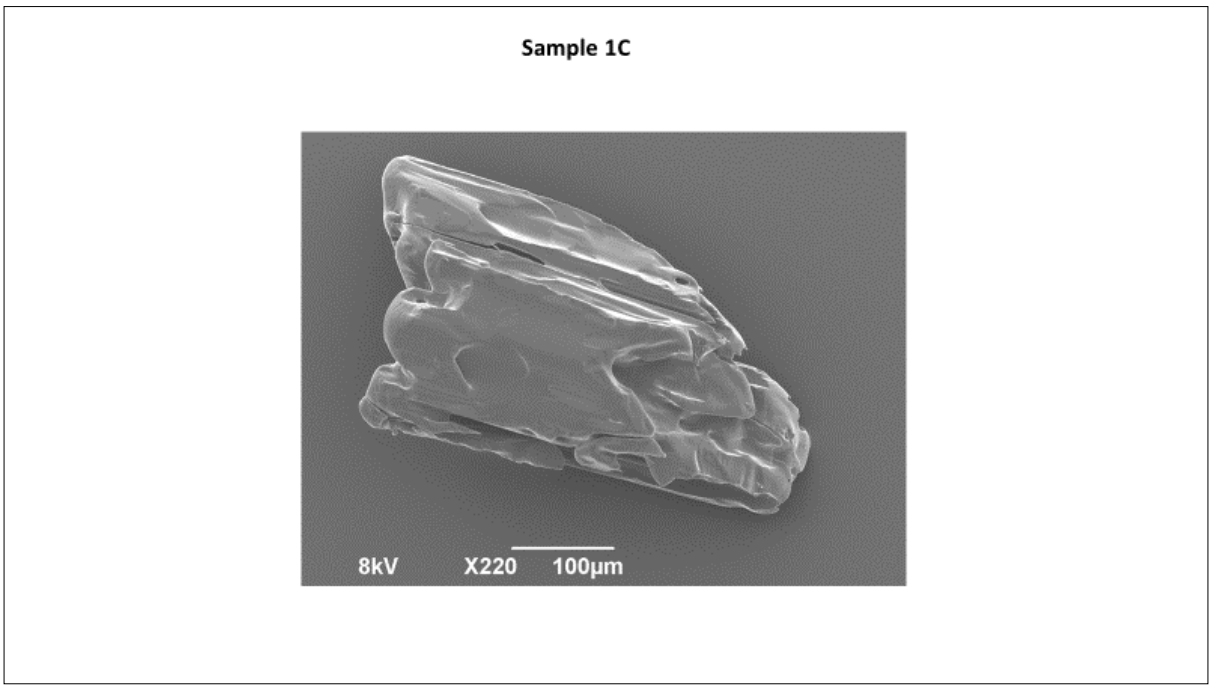

362

363 **Figure 43**

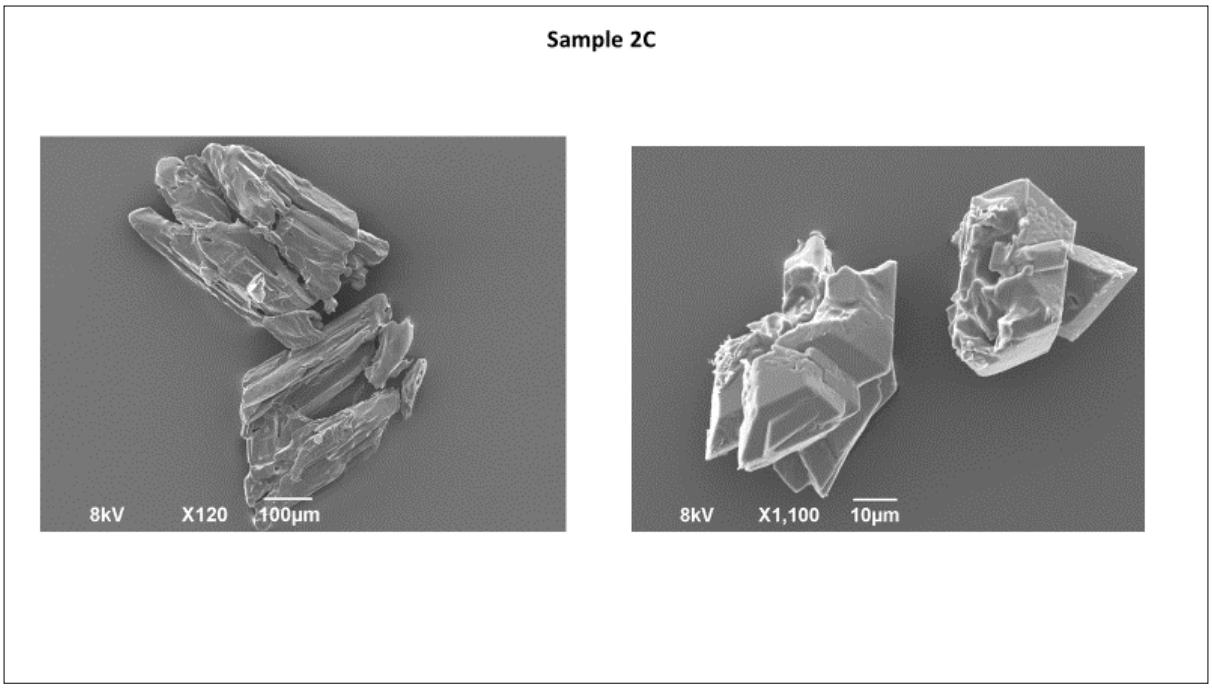

364

365 **Figure 44**

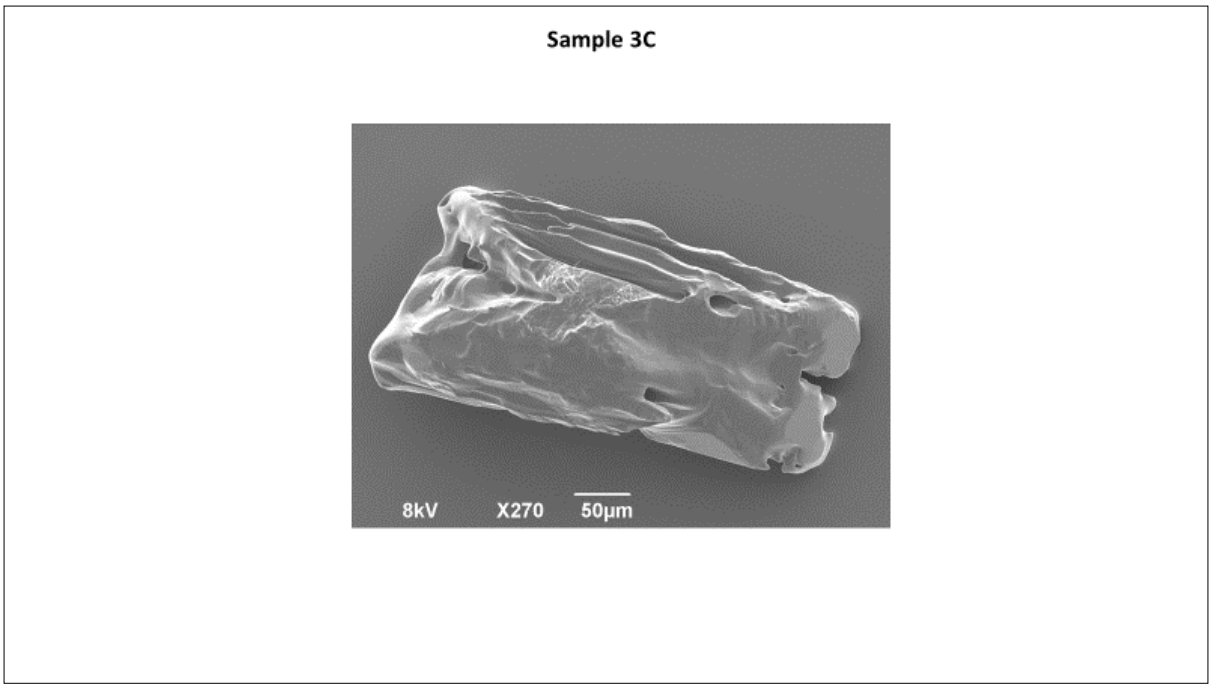

366

367 **Figure 45**

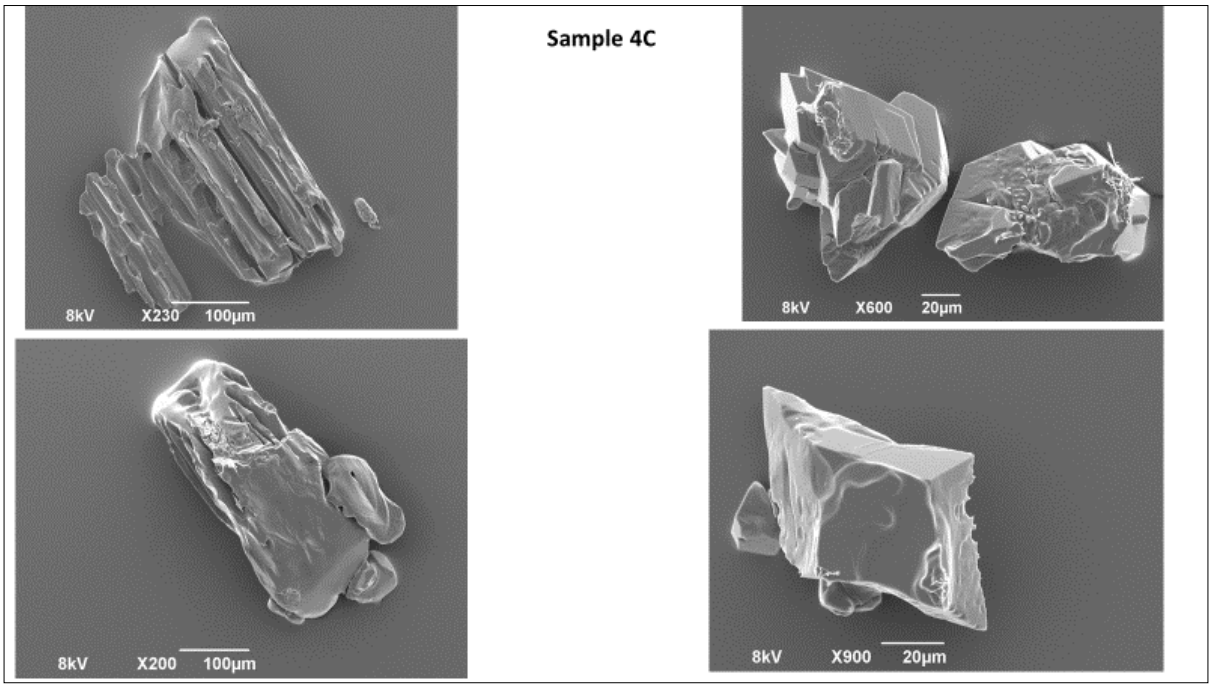

368

369 **Figure 46**

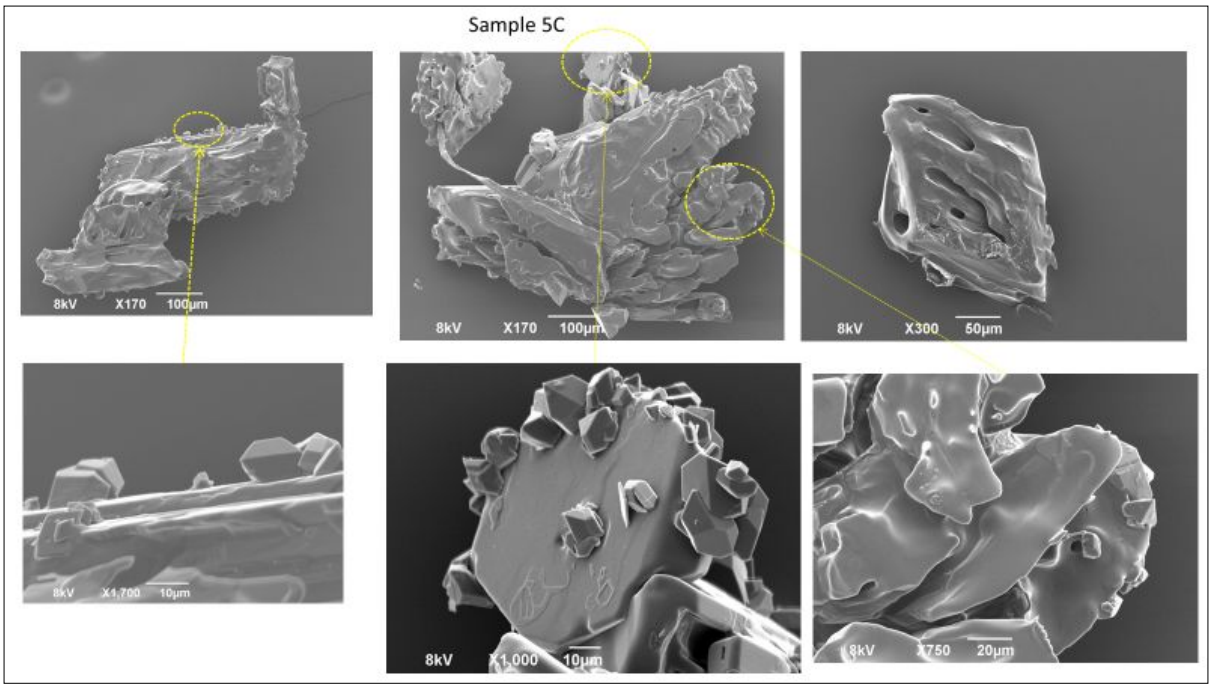

370

371 **Figure 47**

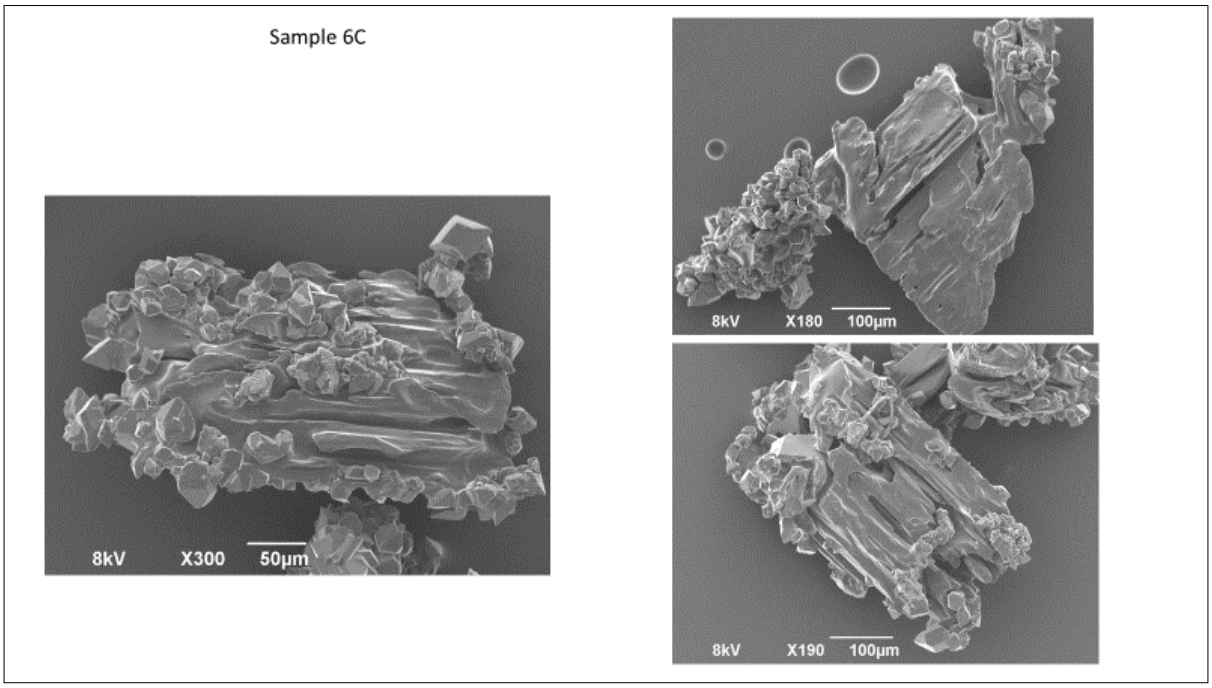

372

373 **Figure 48**

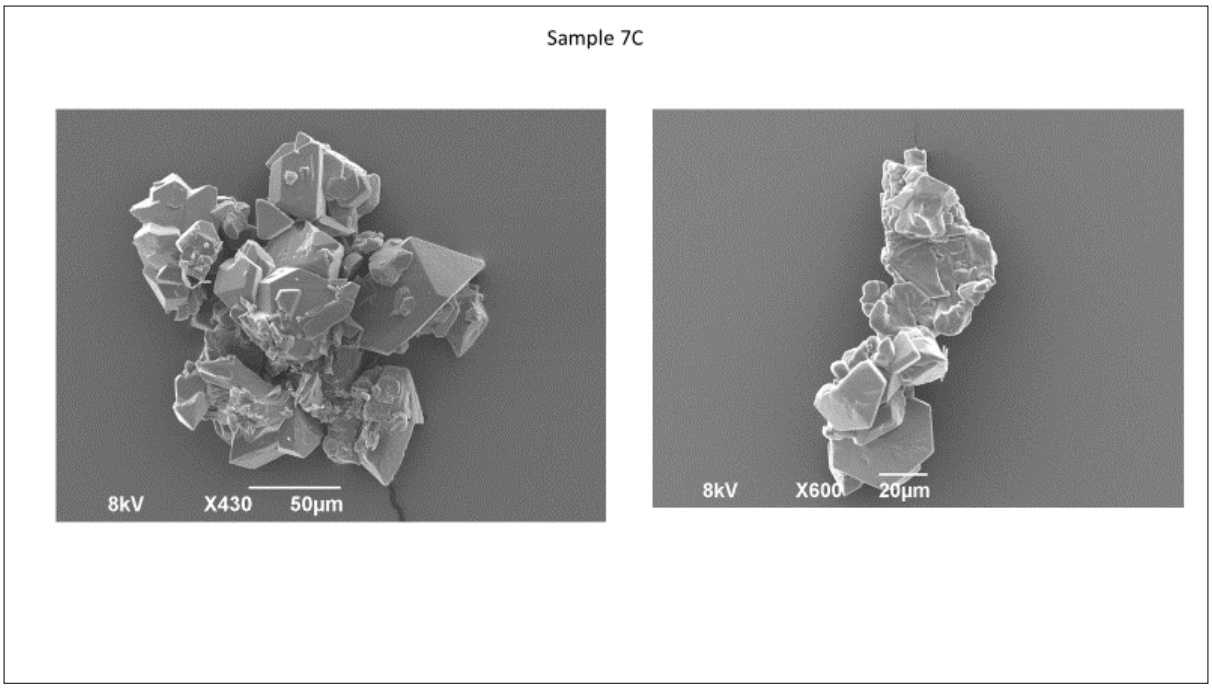

374

375 **Figure 49**

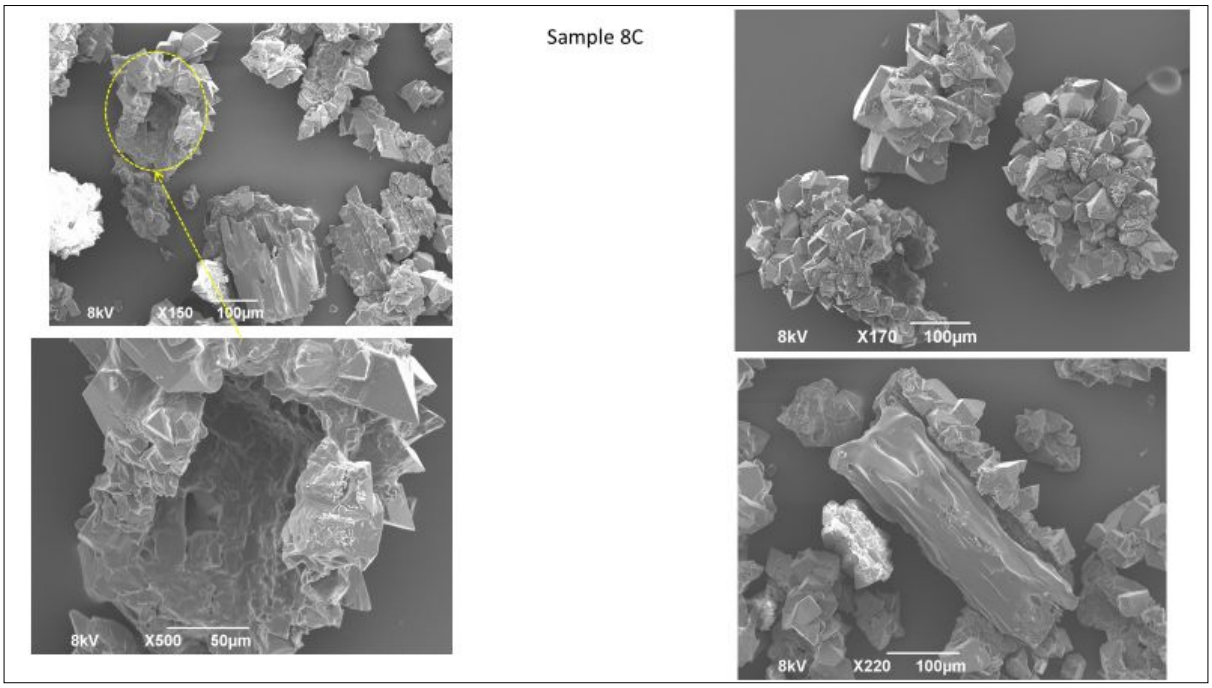

376

377 **Figure 50**

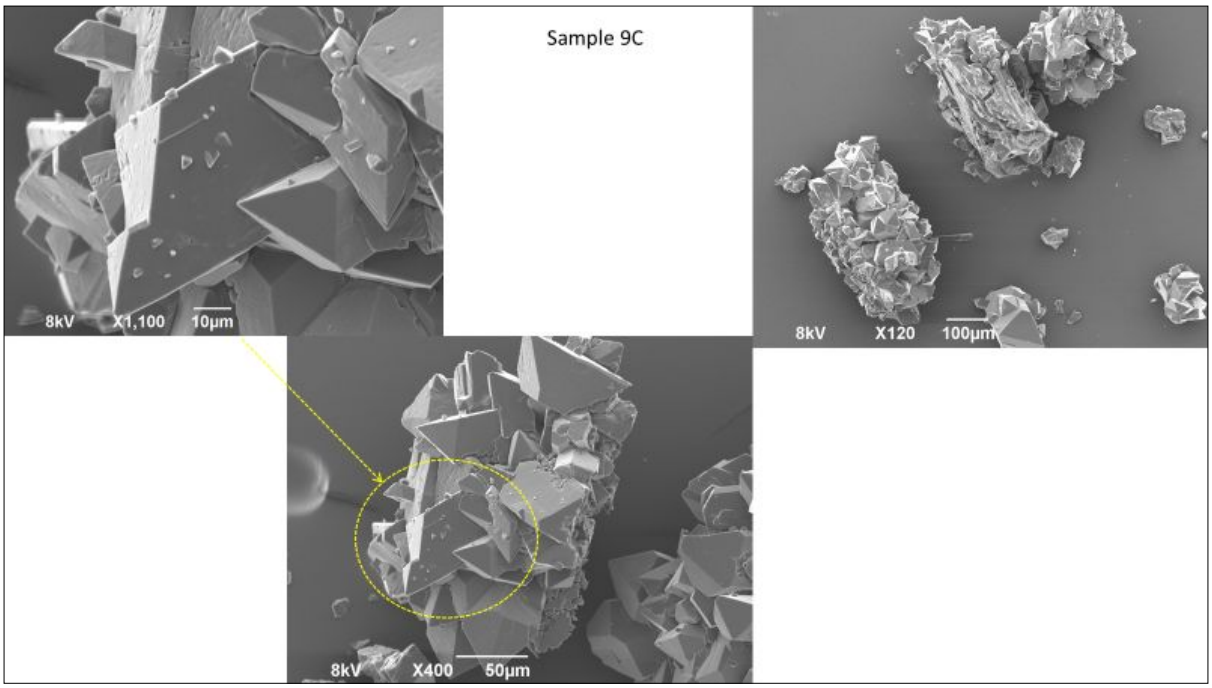

Figure 51

Experiment D

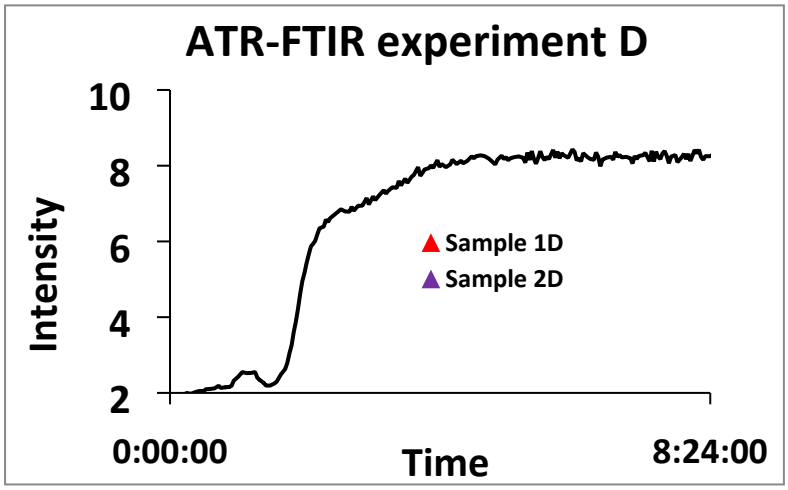

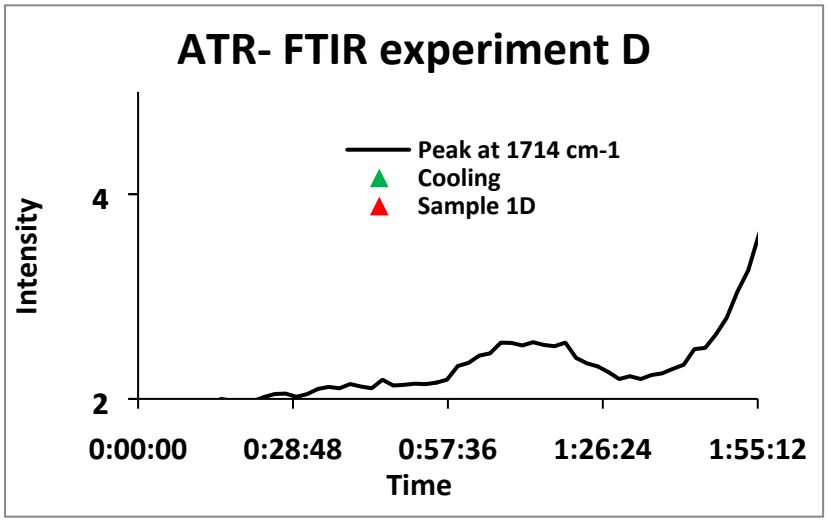

Figure 52 IR data from 250 mL experiment D shows the onset of THP concentration decay at time 1:19:26. Sample 1D was taken at 1:27:26 and sample 2D at time 8:20:00.

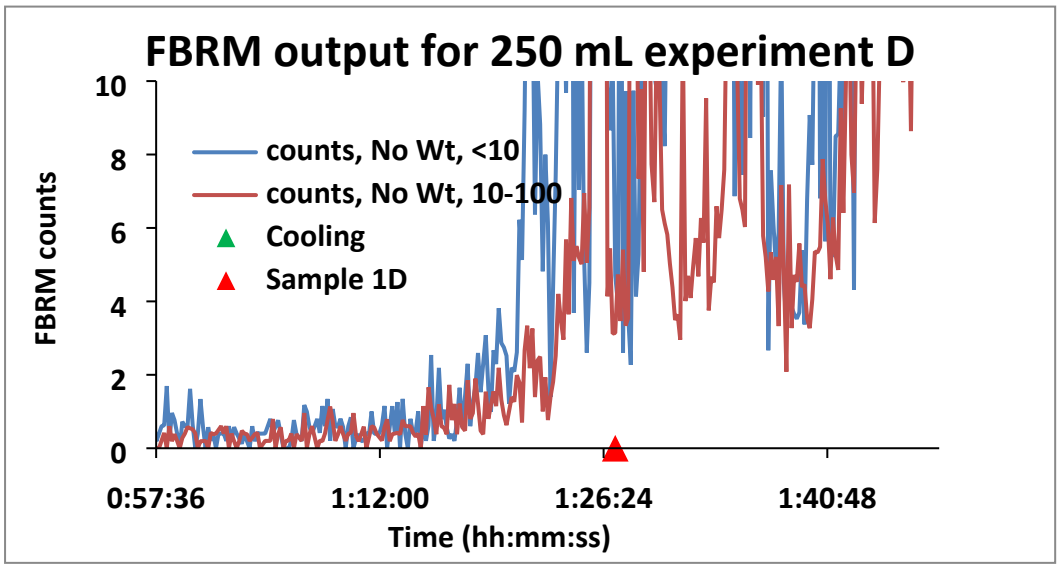

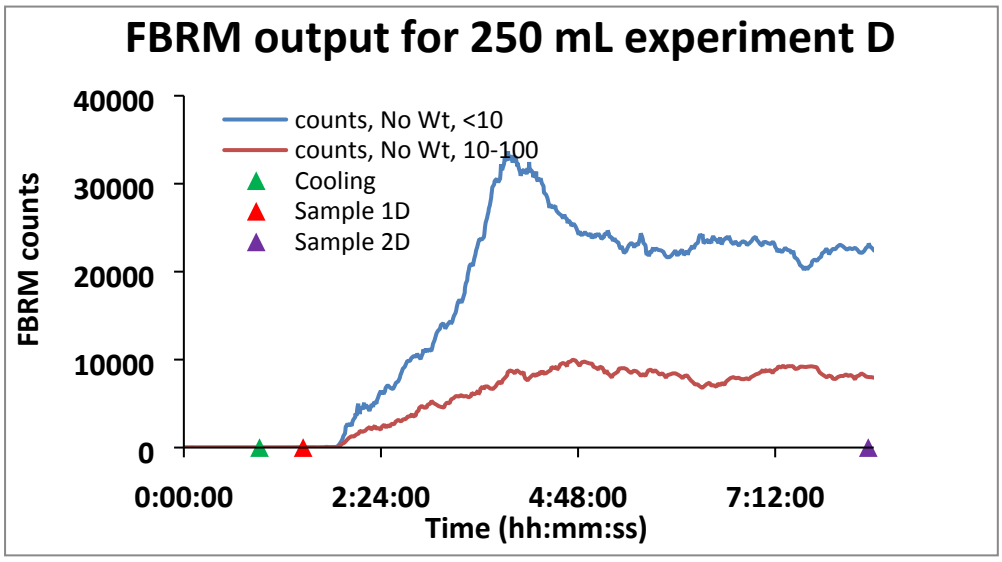

Figure 53 FBRM data collected from 250 mL experiment D. Particle detection began to increase at time 1:15:18.

Experiment D was performed over 9 hours and two samples were taken. Sample 1D was taken at time 1:27:26 and PXRDs revealed a pattern closely resembling β-GLU. Sample 2D taken at time 8:20:00 shows total transformation to cocrystal.

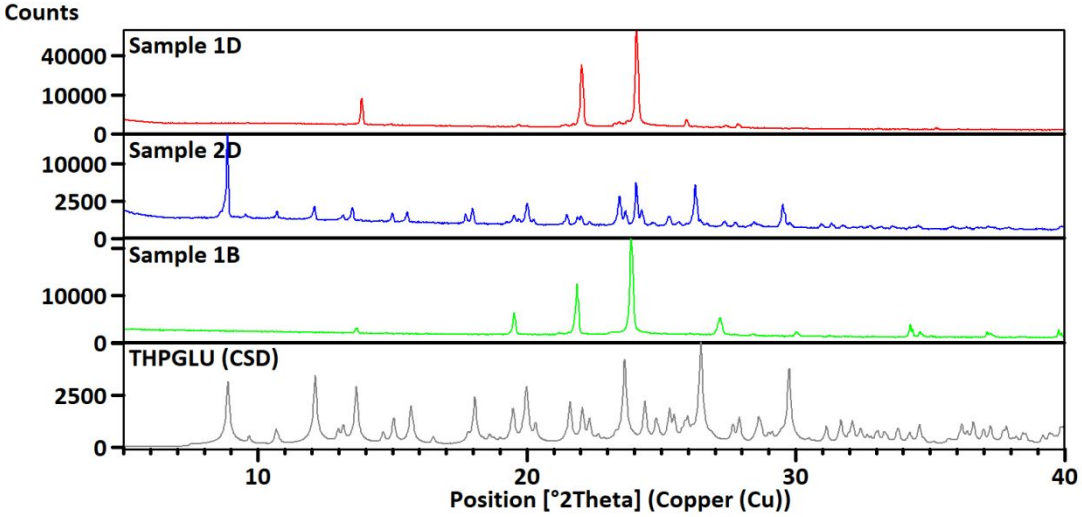

Figure 54 Diffractograms showing that sample 1D is the β-GLU phase as seen in sample 1B and sample 2D is pure THP:GLU cocrystal.

Seeded Experiment

Upon seeding with β-GLU, the number of counts for all particle size ranges increases due to the varying particle size of β-GLU seeds (unsieved), **Figure 55**. ATR-FTIR analysis, **Figure 56**, detected a concentration decrease of THP in solution (t=00:41:25) shortly after seed addition (t=00:39:25), signifying cocrystal nucleation (verified by PXRD analysis, **Figure 57**, performed on all samples shown in **Figure 56**). This is supported by SEM micrographs (**ESI**) where diamond or square shaped crystals appear on the surface of the seeds. Shortly following seed addition the number of particles in the <10 µm and 10-100 µm size range increases further most likely due to fragmentation, **Figure 55**. From these findings it can be rationalised that the cocrystal nucleates on β-GLU seed material.

The data collected via ATR-FTIR and FBRM is unreliable after t=1:25:00 as the crystals are now adhering to the detectors, however, the solid was still sampled after this time for physical characterisation.

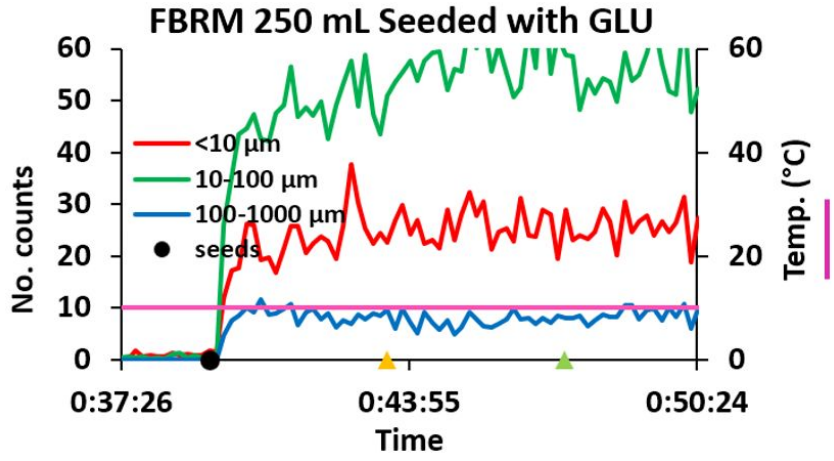

Figure 55 FBRM output for 250 mL seeded crystallisation experiment. Coloured triangles on the x-axis represent time points at which samples were taken.

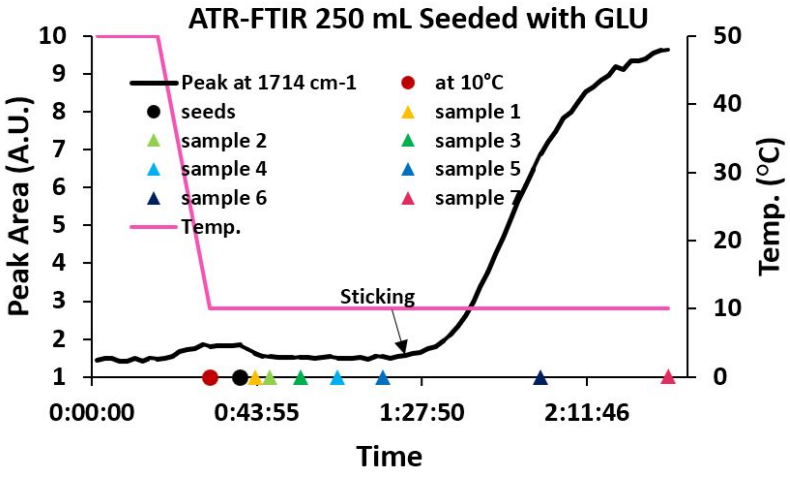

Figure 56 ATR-FTIR from 250 mL crystallisation seeded with GLU.

A total of 7 samples were taken from the seeded experiments from t = 00:43:16 to 02:32:58, the specific times for each sample are in **ESI**. PXRD analysis on the samples display patterns similar to β-GLU with traces of cocrystal up to sample 5, after this the diffractograms display patterns similar to the pure cocrystal with traces of β-GLU (**Figure 57 and ESI**).

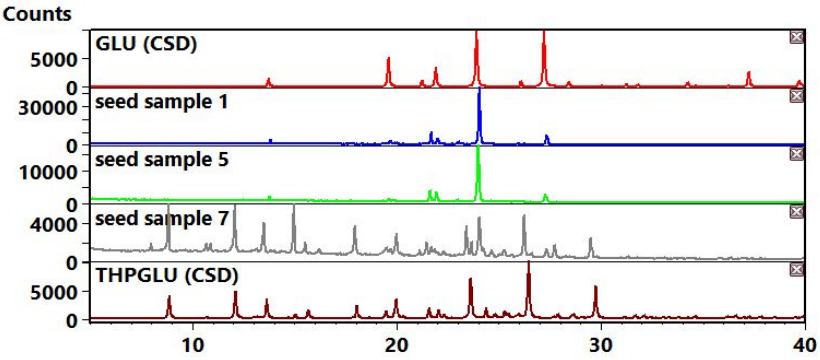

Figure 57 PXRD of selected samples from the seeded experiments compared with the pattern for pure β-glutaric acid (CSD ref. code GLURAC04) and THP:GLU cocrystal (CSD ref. code XEJXIU).

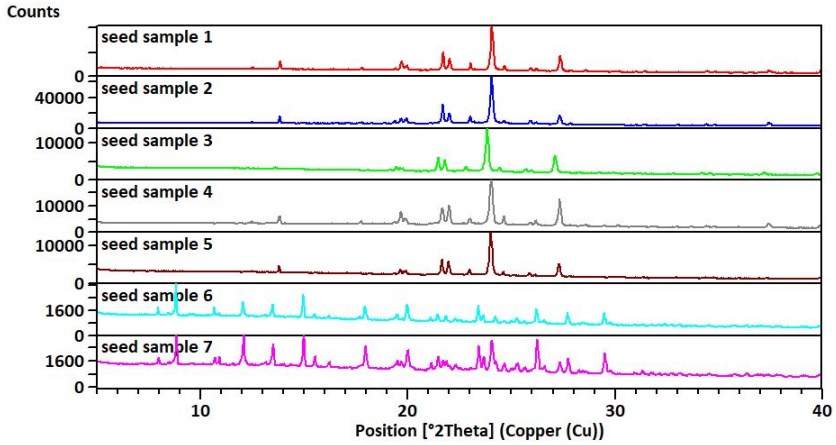

Figure 58 PXRD of samples from 250 mL seeded experiment.

Diffractograms of samples 6 and 7 show mostly THP:GLU cocrystal but some β-GLU remains. There are no PXRD peaks corresponding to pure theophylline in any of the samples 1-7 which can be seen in Figure 59.

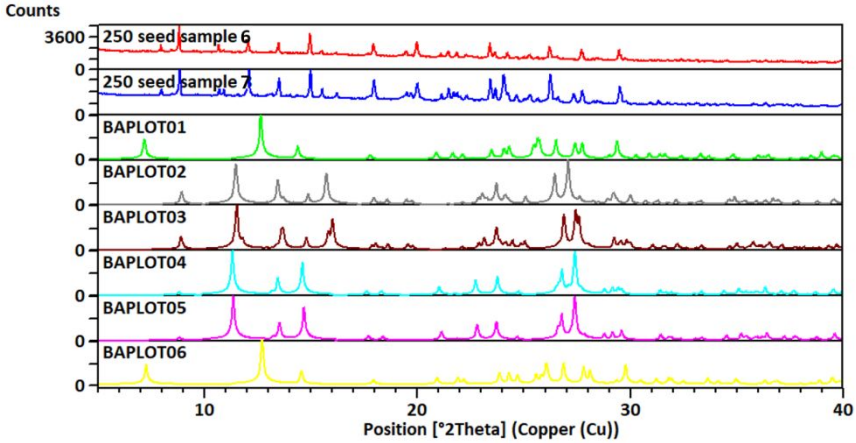

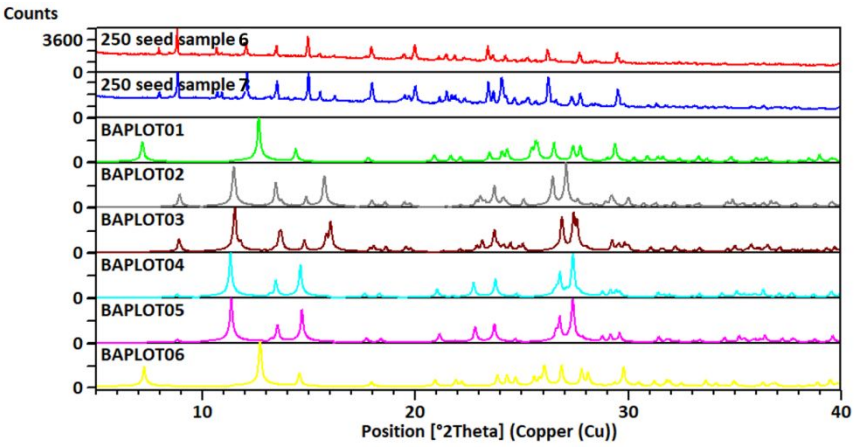

435

436 **Figure 59 PXRD comparing Polymorphs of theophylline (CSD ref.no. BAPLOT0_) to the**
437 **PXRDs of samples taken from the seeded experiment. No pure THP peaks were recorded**
438 **from any of the samples.**

439 .

440 **Table 14 Sample times from 250 mL seeded experiment**

Sample	Time
1	00:43:16
2	00:46:06
3	00:53:57
4	01:04:48
5	01:16:39
6	01:57:24
7	02:32:58

441

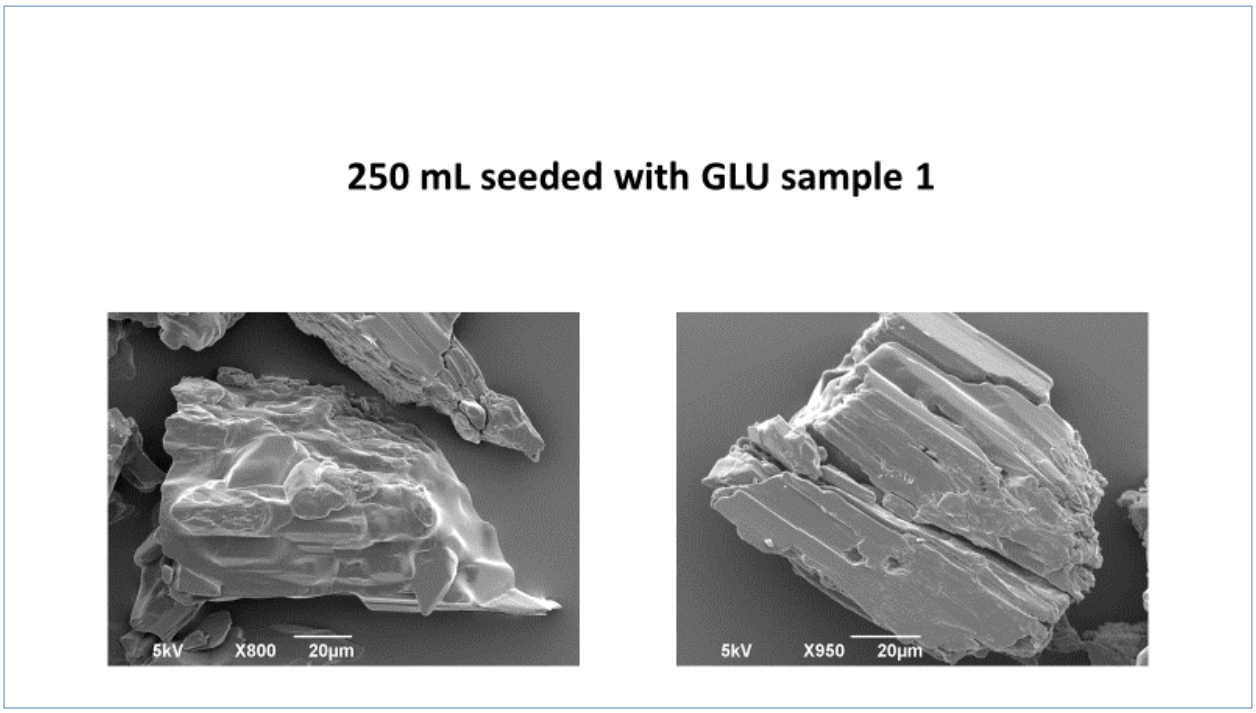

442

443 **Figure 60**

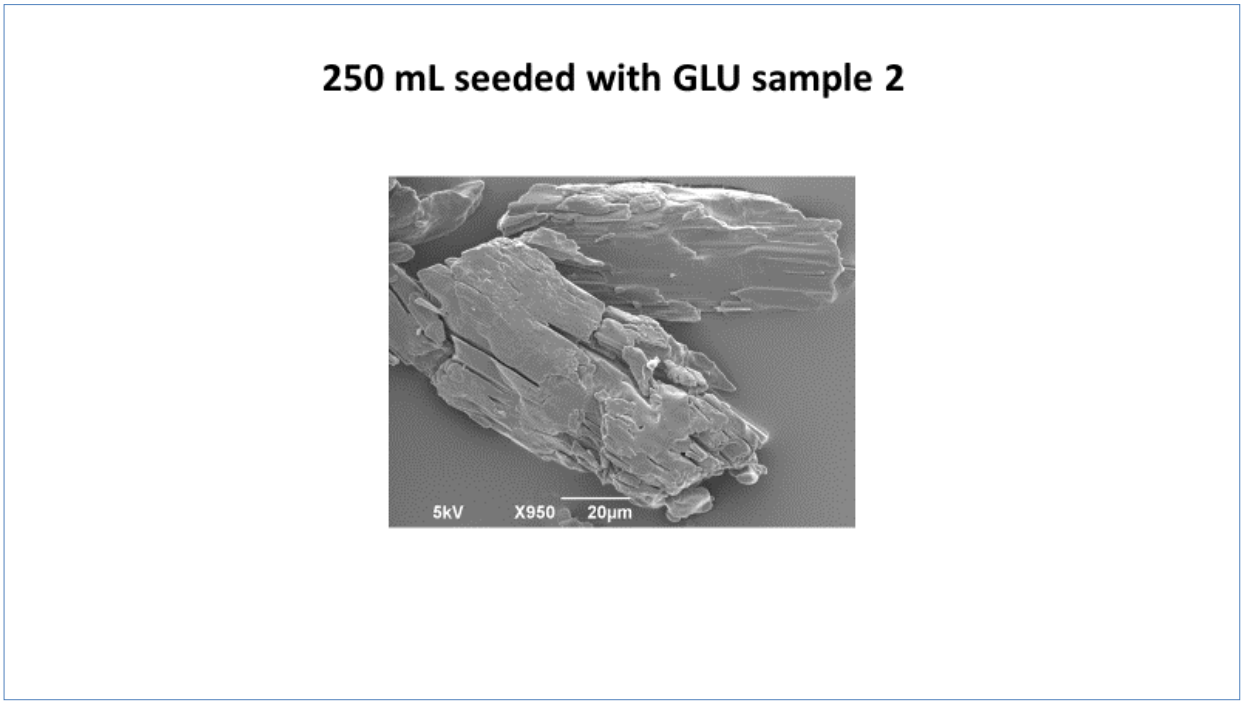

444

445 **Figure 61**

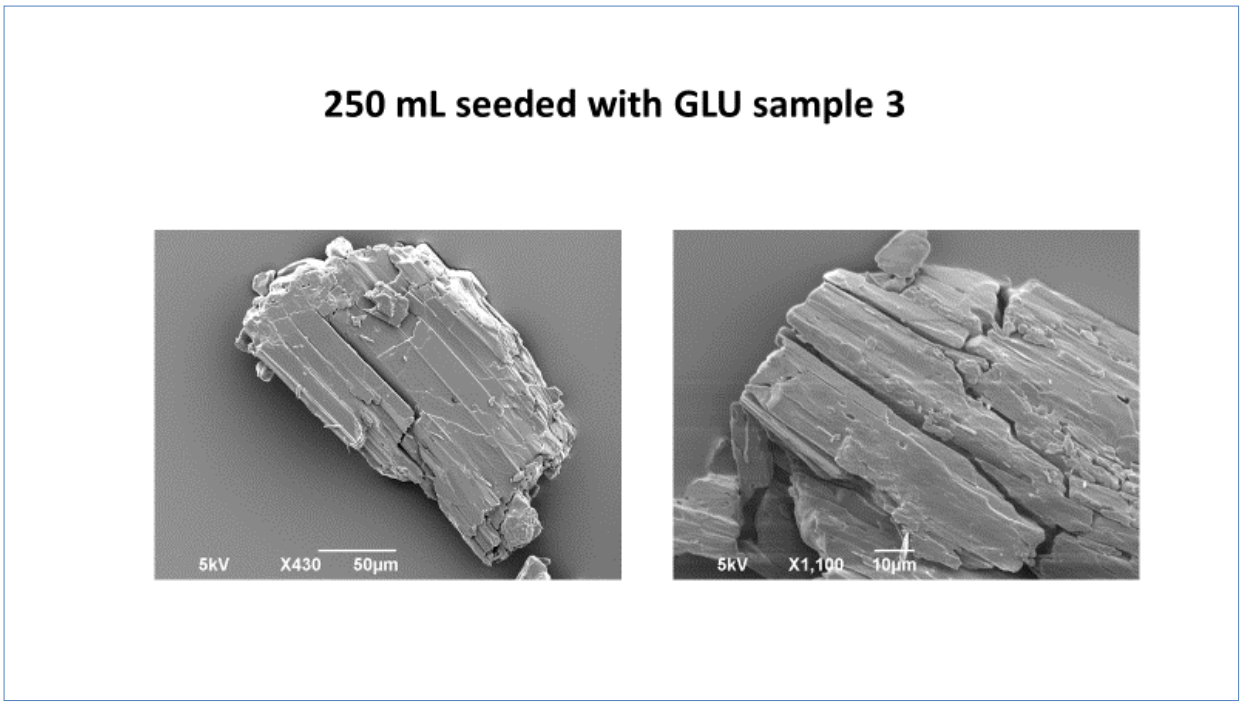

446

447 **Figure 62**

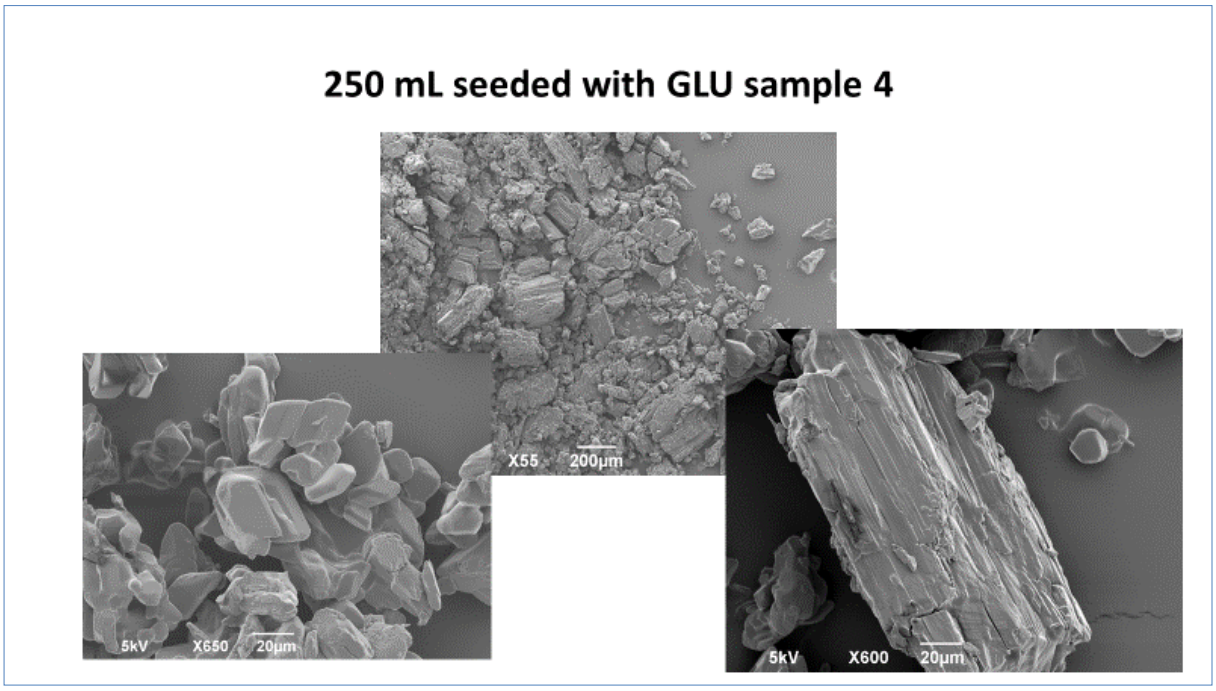

448

449 **Figure 63**

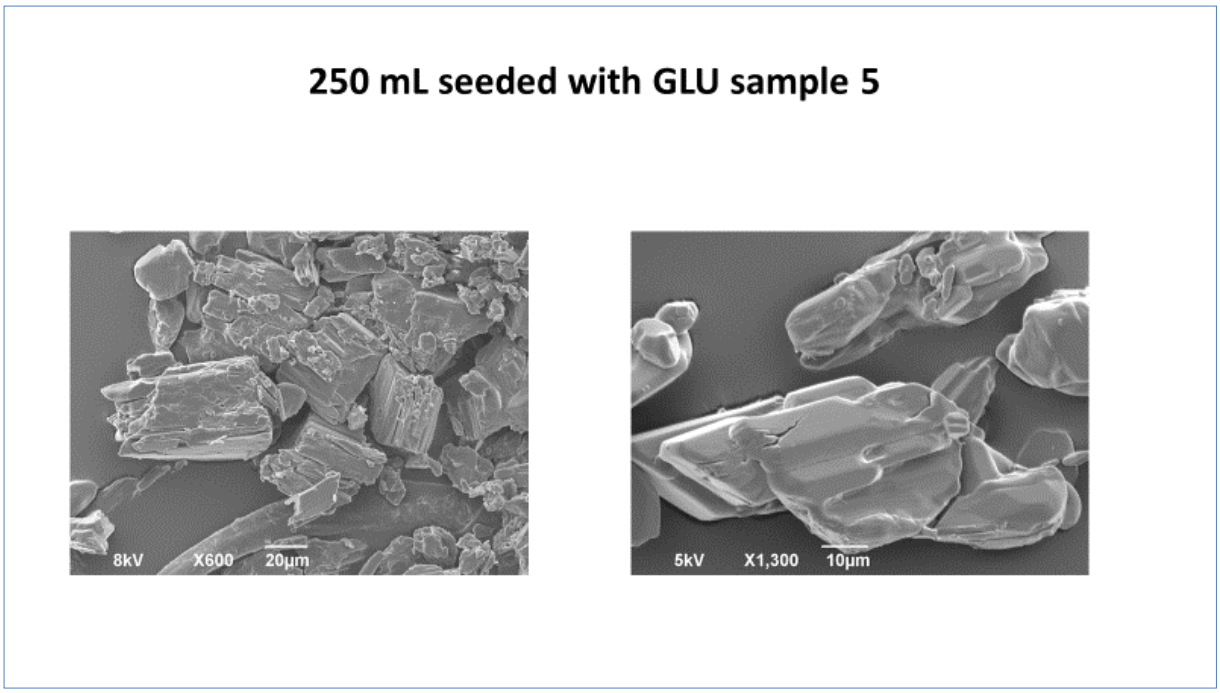

450

451 **Figure 64**

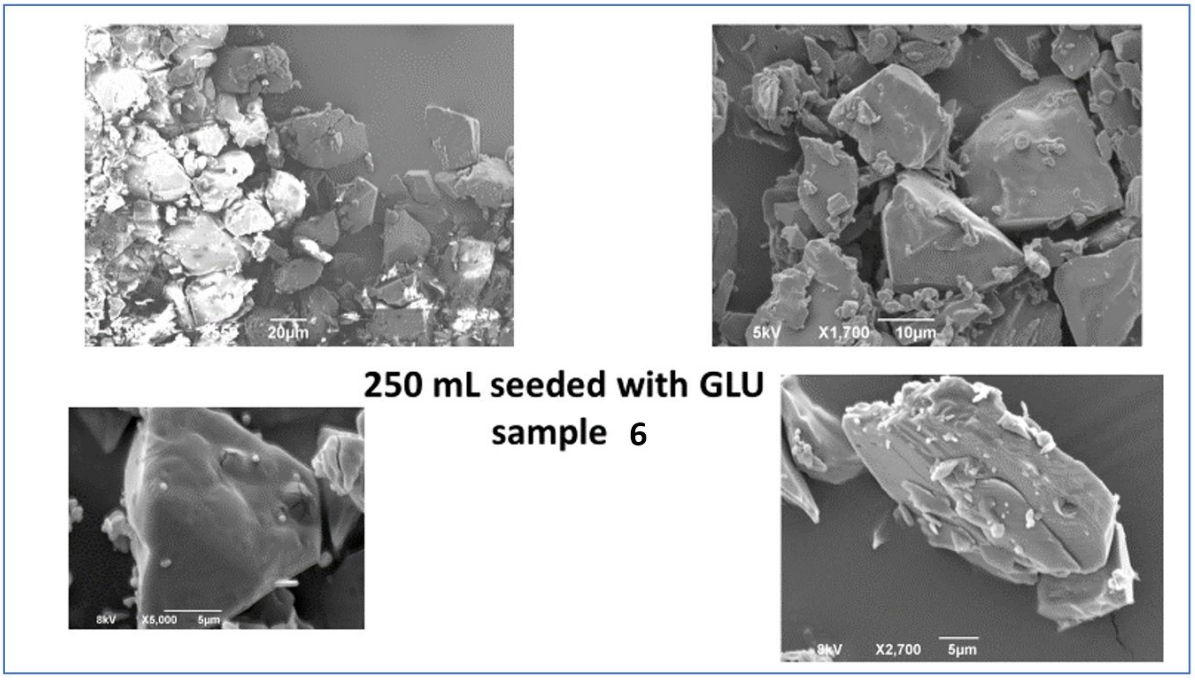

452

453 **Figure 65**

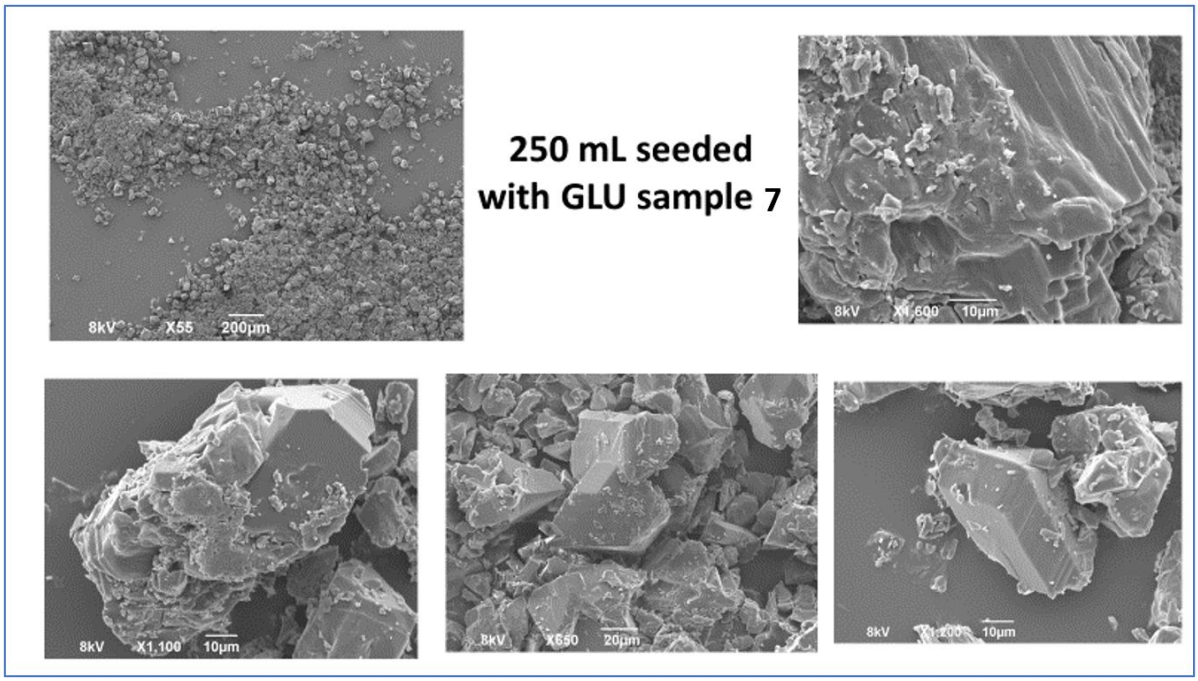

Figure 66

Nucleation analysis

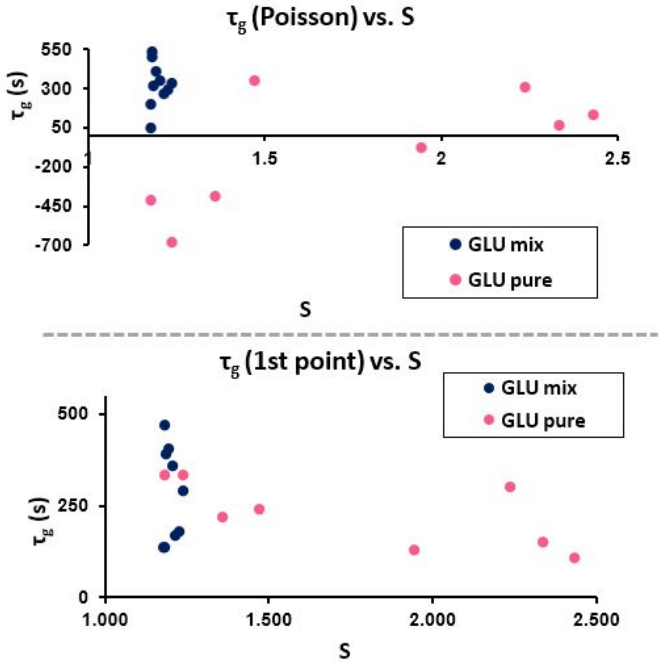

Figure 67Growth rate parameter, obtained by Poisson method or taken as the first nucleation point, versus supersaturation for GLU mix and GLU pure.

Accounting for τ_g (as first point)

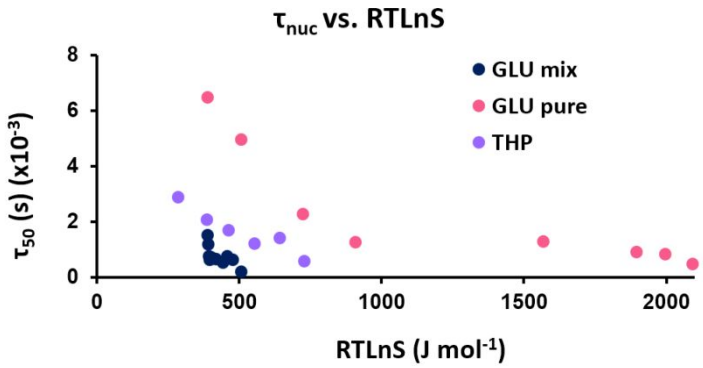

Figure 68 Nucleation of β-GLU from a pure GLU solution and solution containing stoichiometric mixture of THP:GLU (GLU mix) and nucleation of THP II from a pure THP solution from previous work[3], accounting for τ_g.

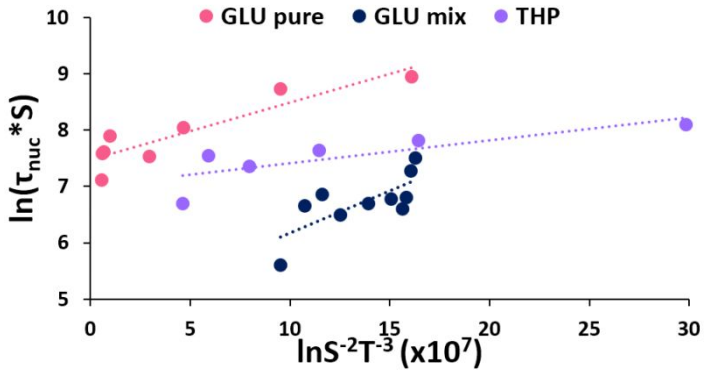

Figure 69 CNT plot from the nucleation times of β-GLU from a pure solution (GLU pure), β-GLU from a stoichiometric mixture of THP and GLU (GLU mix) and pure THP[3], accounting for τ_g.

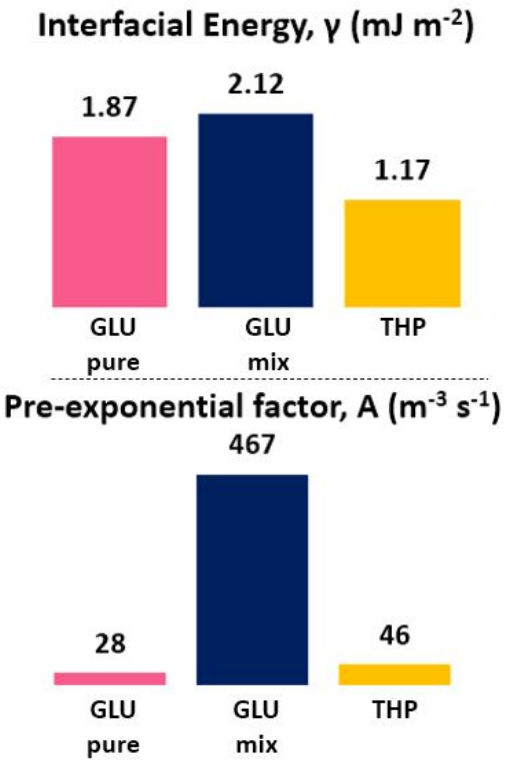

Figure 70 Interfacial energy and pre-exponential factors calculated for GLU pure and GLU mix systems from the CNT plot when τ_g is accounted for.

Table 15 Supersaturation, equilibrium concentration (C_e) and the corresponding pre-exponential factors calculated according to Eq [8] and [9] in the main text for THP II nucleation from previous work.[3]

THP II			
S	**C_e mol m^{-3}**	***A*, Volume-diffusion (m^{-3} s^{-1}, x10^8)**	***A*, Interface-transfer (m^{-3} s^{-1}, x10^8)**
1.13	17.36	20.4	27.6
1.18	17.36	27.6	27.6
1.22	17.36	33.1	27.6
1.27	17.36	39.8	27.6
1.31	17.36	45.0	27.6
1.36	17.36	51.2	27.6

Bibliography

(1) Cardew, P. T.; Davey, R. J. The Kinetics of Solvent-Mediated Phase Transformations. *Proc. R. Soc. London. A. Math. Phys. Sci.* **1985**, *398* (1815), 415–428. https://doi.org/10.1098/rspa.1985.0043.

(2) Zhang, S.; Rasmuson, Å. C. Thermodynamics and Crystallization of the Theophylline-Glutaric Acid Cocrystal. *Cryst. Growth Des.* **2013**, *13* (3), 1153–1161. https://doi.org/10.1021/cg3014859.

(3) Mctague, H.; Rasmuson, Å. C. Nucleation of the Theophylline:Salicylic Acid 1:1 Cocrystal. https://doi.org/10.1021/acs.cgd.0c01594.